(2)

NAVAL POSTGRADUATE SCHOOL

Monterey, California

THESIS

DETECTION AND EXPLOITATION OF VIBRATION INDUCED OPTICAL AMPLITUDE MODULATION

by

George R. Scott

December 1985

Thesis Advisor: John P. Powers

Approved for public release; distribution unlimited

SECURITY CLASSIFICATION OF THIS PAGE

REPORT DOCUMENTATION PAGE

1a. REPORT SECURITY CLASSIFICATION UNCLASSIFIED	1b. RESTRICTIVE MARKINGS
2a. SECURITY CLASSIFICATION AUTHORITY	3. DISTRIBUTION / AVAILABILITY OF REPORT Approved for public release; distribution unlimited
2b. DECLASSIFICATION / DOWNGRADING SCHEDULE	
4. PERFORMING ORGANIZATION REPORT NUMBER(S)	5. MONITORING ORGANIZATION REPORT NUMBER(S)
6a. NAME OF PERFORMING ORGANIZATION Naval Postgraduate School 6b. OFFICE SYMBOL (*If applicable*) Code 62	7a. NAME OF MONITORING ORGANIZATION Naval Postgraduate School
6c. ADDRESS (*City, State, and ZIP Code*) Monterey, California 93943-5100	7b. ADDRESS (*City, State, and ZIP Code*) Monterey, California 93943-5100
8a. NAME OF FUNDING / SPONSORING ORGANIZATION 8b. OFFICE SYMBOL (*If applicable*)	9. PROCUREMENT INSTRUMENT IDENTIFICATION NUMBER
8c. ADDRESS (*City, State, and ZIP Code*)	10. SOURCE OF FUNDING NUMBERS PROGRAM ELEMENT NO. / PROJECT NO / TASK NO / WORK UNIT ACCESSION NO

11. TITLE (*Include Security Classification*)
DETECTION AND EXPLOITATION OF VIBRATION INDUCED OPTICAL AMPLITUDE MODULATION

12. PERSONAL AUTHOR(S)
Scott, George R.

13a. TYPE OF REPORT	13b. TIME COVERED	14. DATE OF REPORT (*Year, Month, Day*)	15. PAGE COUNT
Master's Thesis	FROM _____ TO _____	December 1985	77

16. SUPPLEMENTARY NOTATION

17. COSATI CODES			18. SUBJECT TERMS (*Continue on reverse if necessary and identify by block number*)
FIELD	GROUP	SUB-GROUP	Satellite Damage Assessment, Optical Vibration Sensing Optical Amplitude Modulation, Acoustic Sensing

19. ABSTRACT (*Continue on reverse if necessary and identify by block number*)

The remote sensing of surface vibrations on an object via optical methods has many applications. Current techniques use phase coherent methods which are difficult to apply against a noncooperative target, or one at great distances. A simple method of exploiting the apparent amplitude modulation imposed on a light beam reflecting from a vibrating surface is explored. This method requires no phase reference between source and detector, and can use reflected sunlight as its sensor beam. The design and construction of an experimental receiver is presented, and its sensitivity against targets of varying reflectivity, specularity, and mechanical compliance is tested. Impact detection at a distance using this technique is demonstrated, as is identification of the impacted object from its recovered acoustic spectrum. Theoretical range curves are developed, and suggestions for additional uses of the technology are discussed.

20. DISTRIBUTION / AVAILABILITY OF ABSTRACT ☒ UNCLASSIFIED/UNLIMITED ☐ SAME AS RPT ☐ DTIC USERS	21. ABSTRACT SECURITY CLASSIFICATION UNCLASSIFIED
22a. NAME OF RESPONSIBLE INDIVIDUAL John P. Powers	22b. TELEPHONE (*Include Area Code*) (408) 646-2679 22c. OFFICE SYMBOL 62Po

DD FORM 1473, 84 MAR 83 APR edition may be used until exhausted
All other editions are obsolete

SECURITY CLASSIFICATION OF THIS PAGE

Approved for public release; distribution unlimited

Detection and Exploitation of Vibration Induced Optical Amplitude Modulation

by

George R. Scott
Lieutenant, United States Navy
B.S., Jacksonville University, 1979

Submitted in partial fulfillment of the
requirements for the degree of

MASTER OF SCIENCE IN ELECTRICAL ENGINEERING

from the

NAVAL POSTGRADUATE SCHOOL
December, 1985

Author: George R. Scott
George R. Scott

Approved by:
John P. Powers, Thesis Advisor

Allen E. Fuhs, Second Reader

Harriett B. Rigas, Chairman,
Department of Electrical and Computer Engineering

John N. Dyer,
Dean of Science and Engineering

ABSTRACT

The remote sensing of surface vibrations on an object via optical methods has many applications. Current techniques use phase coherent methods which are difficult to apply against a noncooperative target, or one at great distances. A simple method of exploiting the apparent amplitude modulation imposed on a light beam reflecting from a vibrating surface is explored. This method requires no phase reference between source and detector, and can use reflected sunlight as its sensor beam. The design and construction of an experimental receiver is presented, and its sensitivity against targets of varying reflectivity, specularity, and mechanical compliance is tested. Impact detection at a distance using this technique is demonstrated, as is identification of the impacted object from its recovered acoustic spectrum. Theoretical range curves are developed, and suggestions for additional uses of the technology are discussed.

TABLE OF CONTENTS

LIST OF FIGURES

I. INTRODUCTION

The ability to sense vibrations remotely, in an object of interest, has numerous military and industrial applications ranging from intelligence gathering to non-invasive machine health determinations. Traditional methods of noncontact vibration sensing include passive sonar, direct acoustic measurements in air, and various optical methods. This paper will explore the potential of one simple optical technique.

There are several methods currently in use for optical vibration sensing (OVS) such as direct interferometry, speckle interferometery, time-average holography, and optical Doppler measurements. O'Shea, et al [Ref 1] provides a good overview of the mechanics of these techniques: however, two technical points pertinent to the discussion at hand will be reviewed here.

First, all the current methods of OVS are based on some type of optical heterodyning. This might have to be explicitly designed by the engineer, as in Doppler measurement, or it may be inherent in the optical layout of the sensing system, as in speckle interferometry. In either case the use of a beam of phase coherent light is required, usually generated by a laser of some type.

It is this use of laser light as the target illumination that gives rise to the second point, namely that such methods

are active techniques, in the electronic warfare sense of the word; that is, they all require deliberate illumination of the target with the sensor beam and, conversely, they cannot use any illumination that is already falling on the target to perform the OVS. Indeed, any such ambient illumination is generally considered as noise, and hampers the measurement process.

Another drawback to coherent techniques of OVS is a rather severe range limitation, generally to the coherence length of the illuminating laser. (Although highly specialized lasers may have coherence lengths of a kilometer or more [Ref 1:p. 32] those lasers with sufficient power to perform OVS are typically characterized by coherence lengths measured only in tens of meters.)

This thesis describes a different method of OVS, one which can utilize either a dedicated sensor beam (the "active" mode) or reflected incident illumination (the "semiactive" mode). The theoretical ranges at which this technique can be used are limited only by the sensitivity of the receiver system, and the signal-to-noise ratio of the target's local optical environment.

One possible application of this technique would be the remote monitoring of the vibrational state of a machine in a vacuum, such as a satellite. As an example, a simple receiver and illuminator aboard the Space Shuttle could be used to measure the surface vibrations in a nearby satellite, to

check for proper post-deployment operation in the absence of telemetry (such as occurred in the recent Hughes LEASAT failure) or to determine if exhaust plumes from the orbiter's propulsion system were impinging on a docking target.

The approach described in this paper is based on exploiting the amplitude modulation (AM) which is usually impressed on a light beam reflecting from a vibrating surface. As is noted in Chapter Two, this technique has been known for at least a hundred years, however certain drawbacks in its use have limited research in this area since the end of World War II.

Sensing surface vibrations in this manner does have many drawbacks compared to the phase coherent methods previously touched on. Specifically, the ability to accurately measure vibrational surface excursions, map out vibrational nodes, and sense extremely minute vibrations would be difficult, if not impossible with this method. The advantages of simple AM detection are quite attractive, however. The object need not be illuminated with coherent radiation, and the illumination may take the form of a beam transmitted by the researcher (as is done in this study) or may be reflected ambient illumination. Since a distinct phase reference is not needed between the target and the detector, measurement may take place over long distances, and through phase distorting mediums. Finally, the equipment is, in principle, extremely simple and inexpensive compared to the phase coherent systems.

In the chapters that follow, the design and construction of the receiver used to test this detection technique will be explained, and the results of several experiments presented. The goal of this experimentation was to remotely detect the vibrations in several geometrically simple test objects subject to mechanical impact, and to attempt to identify the individual objects based only on the optically detected acoustical spectrum of the resulting impact data.

Other inquiries undertaken were a study of the effect that varying the specularity of the reflecting surface had on the apparent modulation of the beam, the relative efficiency of the various test objects as modulators, and a method of predicting the impact spectral response of a test object using noise excitation.

II. BACKGROUND

One of the simplest schemes for modulating a light beam is amplitude, or intensity, modulation (AM). In this scheme the intensity of the light is varied in direct proportion to the amplitude of the modulating signal. The relative simplicity of both modulation and demodulation using this technique led to its adoption by early researchers in the field of optical communication.

It is surprising to note that the basic principles of optical AM voice communications were well understood over one hundred years ago. Mims [Ref. 2:pp 8-14] provides an interesting account of the early work of Alexander Graham Bell in this area. It is a little remembered fact that Bell was transmitting speech over impressive distances (several hundred feet) nearly twenty years before A. F. Collins made the first radio transmissions; the modulation method used by Bell for these early transmitters formed the basis for the research outlined in this paper.

The most direct method of amplitude modulating a light beam is to modulate the current to an electrical light source. This light source can range from a low power light emitting diode to a multi-kilowatt carbon arc lamp. The lack of power handling devices (such as vacuum tubes) capable of providing the drive current necessary for this scheme forced

early researchers to devise ingenious mechanical modulators which impressed voice modulation on either artificial light, or reflected sunlight.

The simplest mechanism, and that initially used by Bell, was to reflect the beam to be modulated off a thin, flexible mirror. Physical distortions of the mirror's surface, caused by impinging sound waves from the operator's voice, resulted in the reflected beam being "modulated", as its reflected path varied. (It is important to note that the beam did not have its intensity varied per se but, to the distant receiver, the shimmering effect caused by the uniform intensity beam sweeping over the detectors effective aperture caused a virtual amplitude modulation.)

Optical communication languished after this brief heyday at the turn of the century. A small interest was expressed by various military organizations during the World Wars, however the rapid advance of radio technology eclipsed the usefulness of optical communications schemes. Even though the advent of the laser sparked a renewed interest in the field, the line-of-sight restrictions on transmission range still has limited free-space optical links to a few specialized applications.

The primary difference in the optical transmission systems of today and those of a hundred years ago is the type of modulation. Detector technology has, of course, advanced rapidly but the potential for increased range with these

devices would be hard to realize using AM. The simple AM modulator described earlier shows how easy it is to amplitude modulate sunlight. This effect, when caused by mechanisms such as atmospheric turbulence, random reflections off moving machinery, or the presence of vibrating objects in the field of view of the detector, causes various levels of AM noise in the receiver. It was to minimize the effect of such noise that the more sophisticated methods of amplitude invariant modulations were developed. These include several forms of pulse modulation (e.g. pulse position and pulse frequency modulation) and fundamentally different techniques, such as phase and frequency modulation of the light beam itself. (O'Shea provides a good introductory treatment of this subject [Ref. 1: Chapter 8].)

The tremendous range increases made possible by these techniques has resulted in the virtual abandonment of optical AM since the middle fifties, except in systems such as opto-isolators and like, where simplicity is paramount [Ref 3].

It is, however, this very susceptibility to noise that makes the high gain AM optical receiver such a good candidate for vibration sensing. (Note that Bell's early receiver was in essence an OVS device, sensing the vibration levels in a distant transmitter mirror.)

An example of the potential of this technique was noted in passing by a researcher in New Zealand, A. G. Richardson. Although not mentioned in his original paper [Ref 4], Rodgers

[Ref 5] indicates that Richardson was engaged in research on high gain optical receivers for long distance AM reception. Whatever the reason, Richardson was testing such a receiver by exposing its cesium cell sensor to sunlight. (The rumble induced by the passage of clouds was apparently used as an expedient optical signal generator for initial adjustments.) While engaged in this study, Richardson was puzzled by the presence of numerous tone bursts lasting about 100 milliseconds, and varying in frequency from 100 Hz to about 500 Hz. He devised a clever experiment to determine the source of the modulation, and finally concluded that it was caused by the passage of insects through the field of view of the detector. Although invisible to the human eye, the reflection of sunlight from the vibrating wings of the insects imposed an extremely small AC signal on the strong DC sunlight seen by the receiver. That this was easily detected by Richardson's equipment is a hint of the usefulness of this technique.

Interestingly enough, a similar "problem" was encountered by the author in constructing the receiver used in this research. While initially aligning the first successful design, a strong, intermittent buzz of about 30 Hz was noticed in the receiver's output. This interference was eventually correlated with the appearance of a hummingbird at a window feeder located several meters from the receiver. At this point in the construction the receiver was devoid of any

external collecting optics, yet it provided a strong detection of the modulated sunlight reflected from the small bird's wings.

For purposes of this research, the author has assumed that light reflected from any vibrating surface would be similarly modulated to some extent, and that this modulation could be detected by a carefully designed high-gain optical AM receiver.

The anecdotal experiences above also serve to illustrate another fact; the signals produced by this inadvertent AM modulation are generally frequency invariant. That a given target of interest may modulate light with a small, distinct group of frequencies is a powerful asset to the engineer trying to detect them, particularity if their values are known in advance. Even if these frequencies are not known, a spectral display of the AM receiver's output is likely to show the presence of signals of interest more quickly and unambiguously than any other method. This fact was borne out during the author's research, and is somewhat analogous to the effectiveness of "panoramic" displays on electronic warfare equipment.

The usefulness of viewing this problem in the frequency domain cannot be overemphasized. Signals and events in this experimentation, which would have been undetected on a conventional time domain display, or by the human ear, were easily spotted using a sensitive audio frequency spectrum

analyzer. The effects noted in the study of targets subject to impact, which were simple to record and compare in the frequency domain, would have been difficult, if not impossible, to interpret in the time domain.

III. RECEIVER DESIGN AND CONSTRUCTION

A. DESIGN SPECIFICATIONS

Before elaborating on the design and construction of the test receiver, it is necessary to present the specifications used to guide this effort. These specifications are not presented in any special order, however their relative importance is noted in the individual discussions below.

1. Bandwidth

Although useful acoustic measurements can be made in excess of 1 MHz, particularly in machine health diagnosis systems, the bandwidth of the receiver was limited to the audio spectrum (20 Hz to 20 kHz). The primary reason for this limitation was that the receiver was to be interfaced with a Hewlett Packard HP-3285A digital spectrum analyzer. The research to be conducted was heavily dependent on the capabilities of this machine, which is limited to an upper frequency of 20 kHz, hence the receiver was designed with a similar bandwidth. (As will be seen, this did not handicap the experimentation.) An equally important reason to limit the bandwidth was the need for very high gain in the first stage of the amplifier, and the resultant easing of the gain-bandwidth tradeoff problem simplified the design. Finally, limiting the response to the audio frequencies allowed liberal use of bypass capacitors throughout the amplifier,

preventing RF feedback without imposing the usual restrictions on lead dress and component layout, although the latter could not be entirely ignored.

2. Gain

The gain of the receiver was to be as high as possible, given the bandwidth restrictions above. Since the modulation components being sought would be only a tiny AC ripple, the ability to amplify the signal to a useable level would hinge on a relatively high gain, likely in excess of 50 dB. Although predicting the exact gain needed without a priori knowledge of the experimental results was impossible, the assumption was made that the higher the receiver gain, the better. Naturally, low noise components were selected for the first stage of the amplifier to prevent masking the signal of interest with receiver-produced noise.

3. Cost

The cost of the receiver was to be kept to a minimum by using off-the-shelf components for construction. This not only had the laudable benefit of cost reduction, but significantly reduced development time as all components were readily available.

4. Complexity

It was decided that incremental improvements in receiver performance would not be purchased at the price of greatly increased complexity. The design of very high-gain amplifiers is a specialized discipline, and maximizing

receiver performance would necessitate considerable study in this field if a stable design was to be produced. Since the research goals could be accomplished with less than the maximum performance possible by the receiver, a more modest design of good stability was chosen.

5. Optical Bandwidth

The transducer selected for the receiver was to be sensitive to visible (400 nm to 700 nm) wavelengths to simplify the process of optical alignment of the test setup.

B. TRANSDUCER SELECTION

There are numerous optical transducers on the market. A brief summary of each of the more common ones, and their characteristics, is presented below. Particular attention is paid to the detector's parameters that make it suitable or unsuitable for use in an AM optical receiver, and factors not important to this task are ignored. Readers interested in a somewhat more thorough description should consult Mims [Ref. 2: Chap. 4] or the professional literature.

1. Photoresistive Devices

This class of detectors includes devices whose resistance changes as a function of the incident illumination on their sensitive surfaces. A typical example is the cadmium sulfide (CdS) cell. These devices are inexpensive, and relatively sensitive to visible radiation, however they have poor dynamic range (i.e. they are easily "swamped" by strong DC sources) and exhibit undesirable hysteresis.

2. Photomultiplier Tubes

These devices represent the opposite end of the spectrum in detector technology. They have unrivaled sensitivity (down to the single photon level) and extremely fast rise times. Drawbacks include the need for a high voltage bias supply, the physical fragility of the tube, high cost, and an extremely small dynamic range.

3. Phototransistors

These devices are formed by packaging a specially designed transistor in an optically transparent case. They are small, inexpensive, have reasonable rise times, and good sensitivity (particularly in FET or photo-Darlington arrangements). The only drawback for the purpose at hand is the nonlinear gain curve these devices follow, again resulting in saturation at moderate illumination levels and poor dynamic range.

4. Avalanche Photodiodes

Avalanche photodiodes have been referred to as "solid state photomultiplier tubes", and rightly so. They exhibit nearly the same high gain as the photomultiplier tube, but in a smaller, rugged package. Unfortunately they still require several hundred volts of bias and are easily swamped by bright background illumination if not equipped with special filters.

5. PIN Photodiode

The PIN photodiode is so named because of its construction, wherein heavily doped p and n layers of silicon are separated by an undoped (intrinsic) layer. These devices have a sensitivity somewhat lower than that of the phototransistor, but exhibit a very wide dynamic range. They generally give useable signal outputs over a range of several decades of illumination. Photodiodes are also inexpensive, extremely rugged, and produce little noise.

Given the facts above, it was not hard to narrow the detector choice down to the the phototransistor, or the PIN photodiode. Initial experimentation during the receiver construction showed that the low noise of the photodiode, coupled with its broad dynamic range, made it the preferred transducer.

C. RECEIVER FRONT END DESIGN

The PIN photodiode may be considered a variable current source, whose output is proportional to the intensity of the incident illumination. The generally accepted method of amplifying the output of these devices is the use of a sensitive current-to-voltage converter constructed from a high gain, low-noise operational amplifier. The amplifier should have a very high input impedance (to reduce detector loading and hence noise) and a high gain bandwidth product.

The next matter to consider is that of detector bias. The PIN photodiode may be reversed biased, with typical values of

up to 20 volts. This bias voltage has little effect on detector sensitivity, but plays an important role in determining the shunt capacitance of the device, in a manner similar to that of the varicap diode (i.e. varying the width of the depletion region). In circuits designed for extremely fast rise time (on the order of nanoseconds) the diode should be biased at as high a value as possible to minimize the shunt capacitance, and hence minimize high frequency roll off. In the circuit considered here however, this is of little concern and the detector was unbiased for the sake of simplicity.

Using the current-to-voltage convertor shown in the first stage of the receiver schematic diagram (Figure 1), the output of the first stage amplifier (LF 353) can be calculated as:

$$V_1 = R_F * (I_P + I_D)$$

where R_F is the 1 megohm feedback resistor, and I_P is the photo current produced by the diode in response to the incident light. I_D is the so called dark current, and results from a combination of current leakage mechanisms within the diode. This quantity represents the shot and thermal noise levels associated with the device at a given temperature, and hence determines the threshold sensitivity. (The dark

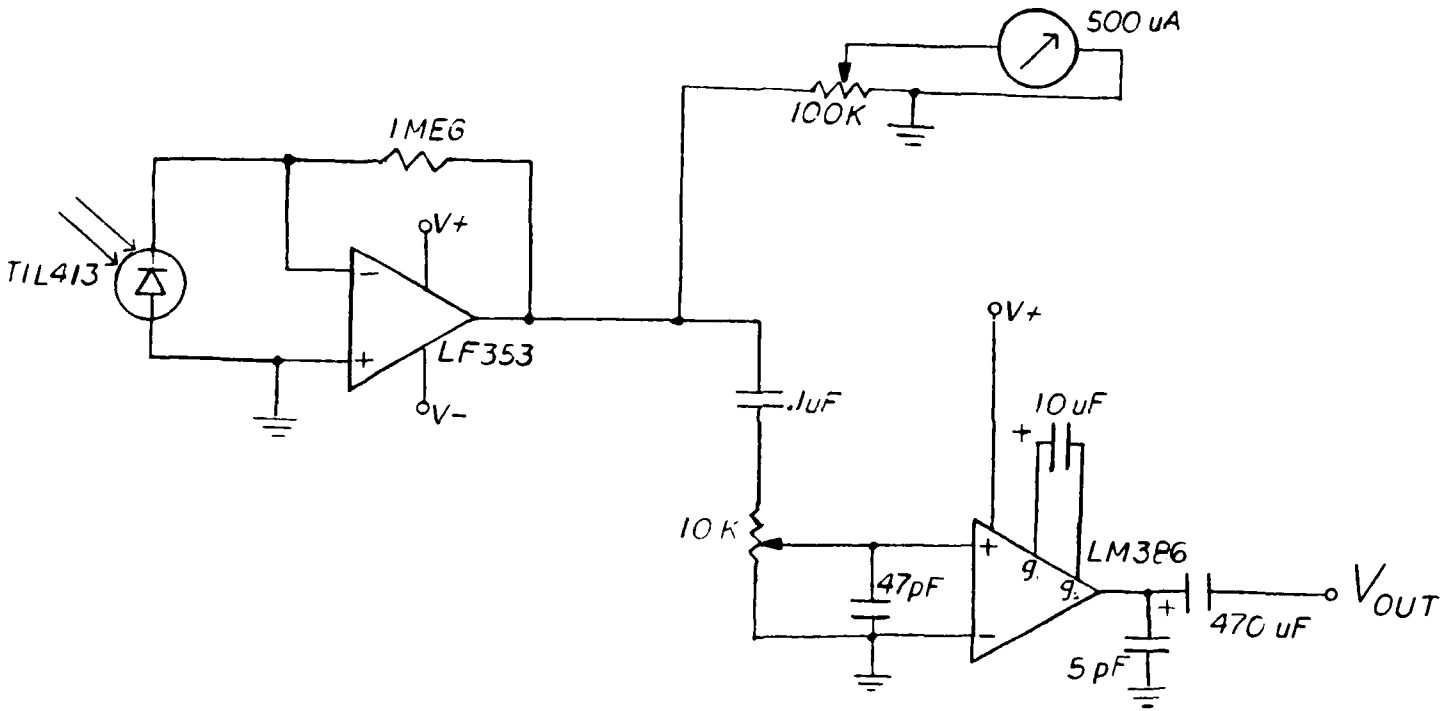

Figure 1. Receiver Schematic

current will be used later in predicting the range of the receiver against a given signal of interest.)

Almost any operational amplifier could have been used for the first stage amplifier, however the LF 353 was chosen because of its high input impedance (10^{12} ohms) and low noise figure (.01 pA/Hz$\cdot^{5}$) compared to other generally available devices. The gain-bandwidth product of 4 MHz was considered sufficient for the demonstration receiver being constructed.

D. RECEIVER SECOND STAGE DESIGN

The second stage of the receiver (Figure 1) was designed around the LM 386 audio power amplifier, configured to give a gain of 46 dB. The operation of this circuit is well documented in numerous design handbooks, and will not be elaborated on here. This particular device was chosen for its low external parts count, and the ability to directly drive a low impedance load such as a speaker. (Initial adjustments to the receiver were made using a speaker to provide audible output, hence the capability to directly drive such a load was convenient.)

The second stage of the receiver was AC coupled to the front end, since only the AC portion of the signal would be of interest in this research. The overall gain of the receiver is adjusted with the 10 K ohm potentiometer that follows the 0.1 uF coupling capacitor.

The complexity of rejecting DC in a current-to-voltage convertor, such as is used here, is considerable; the

compromise of blocking out the DC in the interstage coupling was chosen instead. This procedure does have one drawback however, the photodiode will generate sufficient current to swing the output of the LM 353 to the point of clipping when exposed to bright light, such as specularly reflected sunlight. This effectively locks the receiver up when it is exposed to a very bright scene, even though the photodiode itself may still be operating in a linear fashion. This effect proved to be little practical trouble during the experiments being conducted. However if exposure to very bright backgrounds was expected, the simple addition of a neutral density filter to the receiver's optical path prevented lock up. The 500 uA meter movement connected to the the front end of the receiver was included as an operating aid, indicating the DC level of the front end output. Corrective measures, such as decreasing the target illumination, were taken if the indicated DC level began to approach the front end op amp's positive clipping threshold.

E. RECEIVER CONSTRUCTION AND TESTING

The test receiver was constructed on a small circuit prototyping board, keeping all lead lengths as short as possible (see Figure 2). The detector and power supply (two nine volt batteries) were mounted on the board also to minimize the possibility of feedback and hum pickup. For the collector optics, a small lens constructed of optical plastic

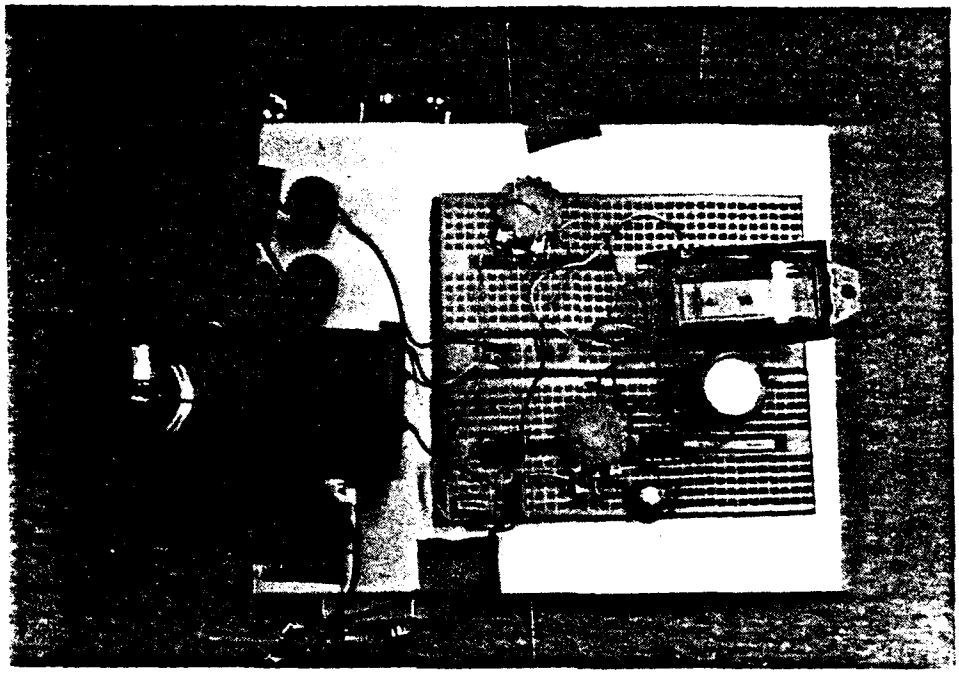

Figure 2. Receiver Layout

was attached to a 35mm film can. The lens used is approximately 2 cm in diameter, with a focal length of 40 mm.

During initial testing, the circuit was noted to be very sensitive, and very prone to breaking into oscillation. The 47 pF bypass capacitor connected to the input of the second stage eliminated this problem. Once the amplifier was operating stably, the two photodiodes obtained for the experiment were connected to the circuit and then installed in the optical housing for testing. The first diode, manufactured by Hewlett Packard as type 5082-4203 performed well, but not nearly as well as the second diode, a Texas Instruments TIL413 which produced about twice the signal-to-noise ratio. This was not surprising since the TIL413 has both a larger active area and roughly twice the responsivity of the 5082-4203. This device was chosen for use in the experiments to follow.

The final problem to be solved revealed itself when the receiver was connected to an oscilloscope. The second stage of the amplifier was oscillating at a frequency of about 250 kHz, causing distortion of the signal waveforms. This problem was eliminated with the installation of a 5 pF capacitor from ground to the second stage output.

To test the overall amplifier frequency response, a voltage divider was constructed from a 10 megohm resistor and a 510 ohm resistor; a signal generator was then coupled via this network to the input of the first stage of the receiver

and the input-output relationships shown in Table I were obtained at the given frequencies. It should be noted that the "gain" calculated is not a true voltage gain for the amplifier, since a current to voltage convertor has no voltage gain defined per se, but rather a transimpedance gain given by the ratio of the output voltage to the input current. However, since this minute input current is difficult to measure directly, and since we are interested only in the relative performance of the amplifier as a function of frequency, these figures will serve adequately. The voltage V_{IN} in Table I is the voltage developed across the 510 ohm resistor in the voltage divider; this voltage was coupled to inverting input of the LF 353. The gain figures presented in the Table are plotted in Figure 3.

The relative change in the amplification, from maximum to minimum, was on the order of 14%. As matters turned out, most of the data of interest was between 100 and 1000 hertz, where the amplifier's response could be considered flat.

A later test of the amplifier using bandlimited white noise and a spectrum analyzer gave essentially the same results as those shown Figure 3.

TABLE I
AMPLIFIER FREQUENCY RESPONSE

Frequency hertz	V_{IN} microvolts	V_{OUT} volts	Gain dB
100	47.7	4.00	98.5
200	47.7	6.00	102.0
300	47.7	6.50	102.7
400	47.7	6.50	102.7
500	47.7	6.50	102.7
600	47.7	6.50	102.7
700	47.7	6.50	102.7
800	46.7	6.20	102.5
900	46.7	6.00	102.2
1000	46.7	5.60	101.6
2000	46.7	4.80	100.3
3000	46.7	3.00	96.2
4000	46.7	2.50	94.6
5000	46.7	2.25	93.7
6000	46.7	2.00	92.6
7000	46.7	1.75	91.5
8000	46.7	1.60	90.7
9000	46.7	1.40	89.6
10000	46.7	1.30	88.9
20000	46.7	1.20	88.2

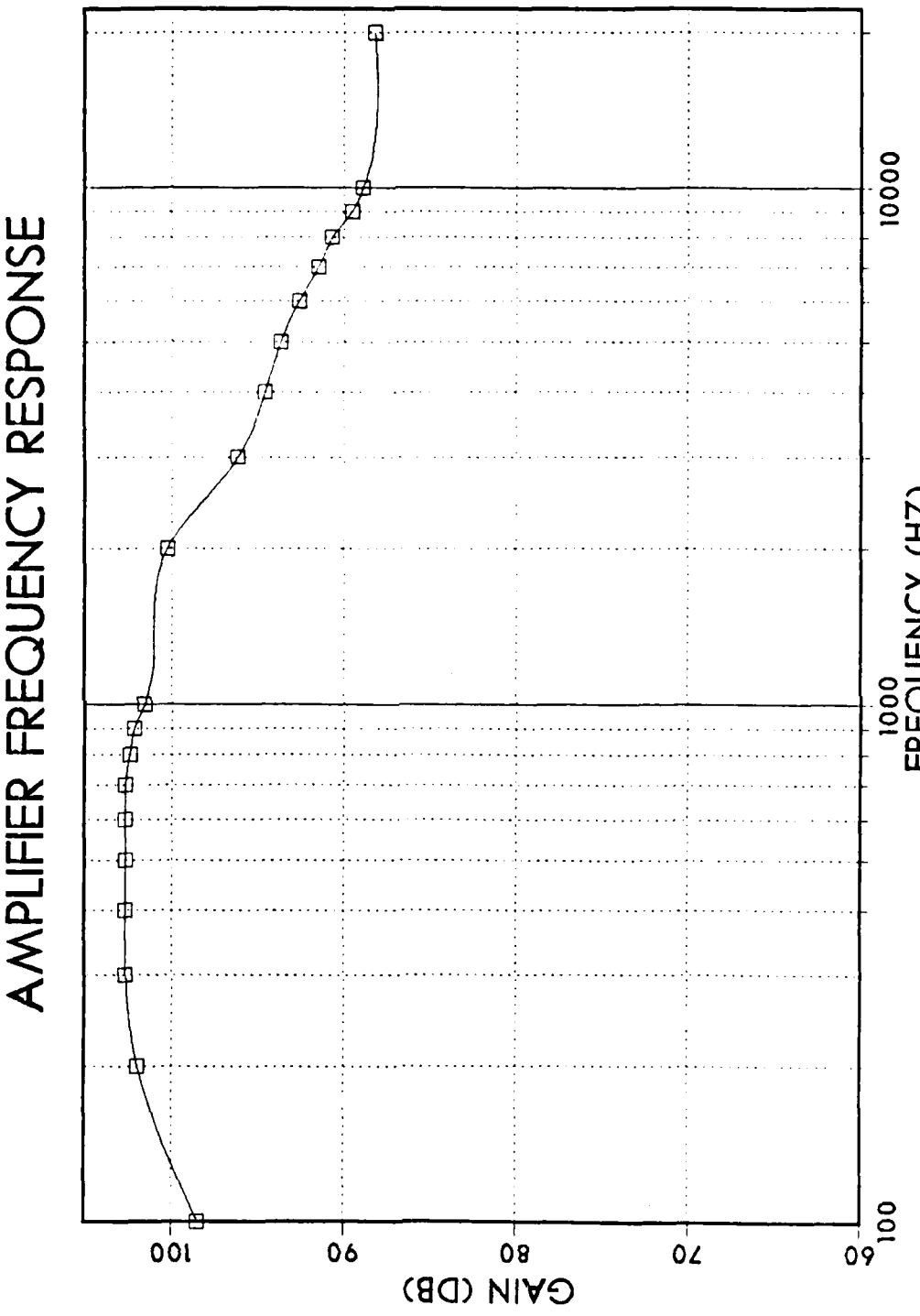

Figure 3. Amplifier Frequency Response

IV. TEST SYSTEM CONFIGURATION

A. TEST SYSTEM LAYOUT

Figure 4 shows the physical layout and data flow in the experiments conducted. The beam from the illuminator (symbolized by a dashed line) was directed at the test object, and the reflection therefrom was intercepted by the receiver. The object-to-illuminator and object-to-receiver distances were fixed at one meter for the experiments described herein. The speaker located behind the test object allowed acoustic excitation using either bandlimited white noise or a single tone. Figure 5 is a photograph of the test layout showing the test object (a mylar disk in this case) and speaker on the left, the illuminator in the right background and the receiver in the right foreground. (The oscilloscope screen on the extreme right shows an actual received signal; the circuit was in operation at the time the photograph was taken).

Signal flow, shown in Figure 4 by solid lines, was straight forward. The received signal was passed to a triggered sweep oscilloscope, and a Hewlett Packard 3582A audio spectrum analyzer. The spectrum analyzer was interfaced to an HP-85 microcomputer, which drove a digital pen plotter for spectrum hardcopy (see Appendix B for a listing of the relevant computer programs). As noted above, the white noise output of the spectrum analyzer was one source of acoustic

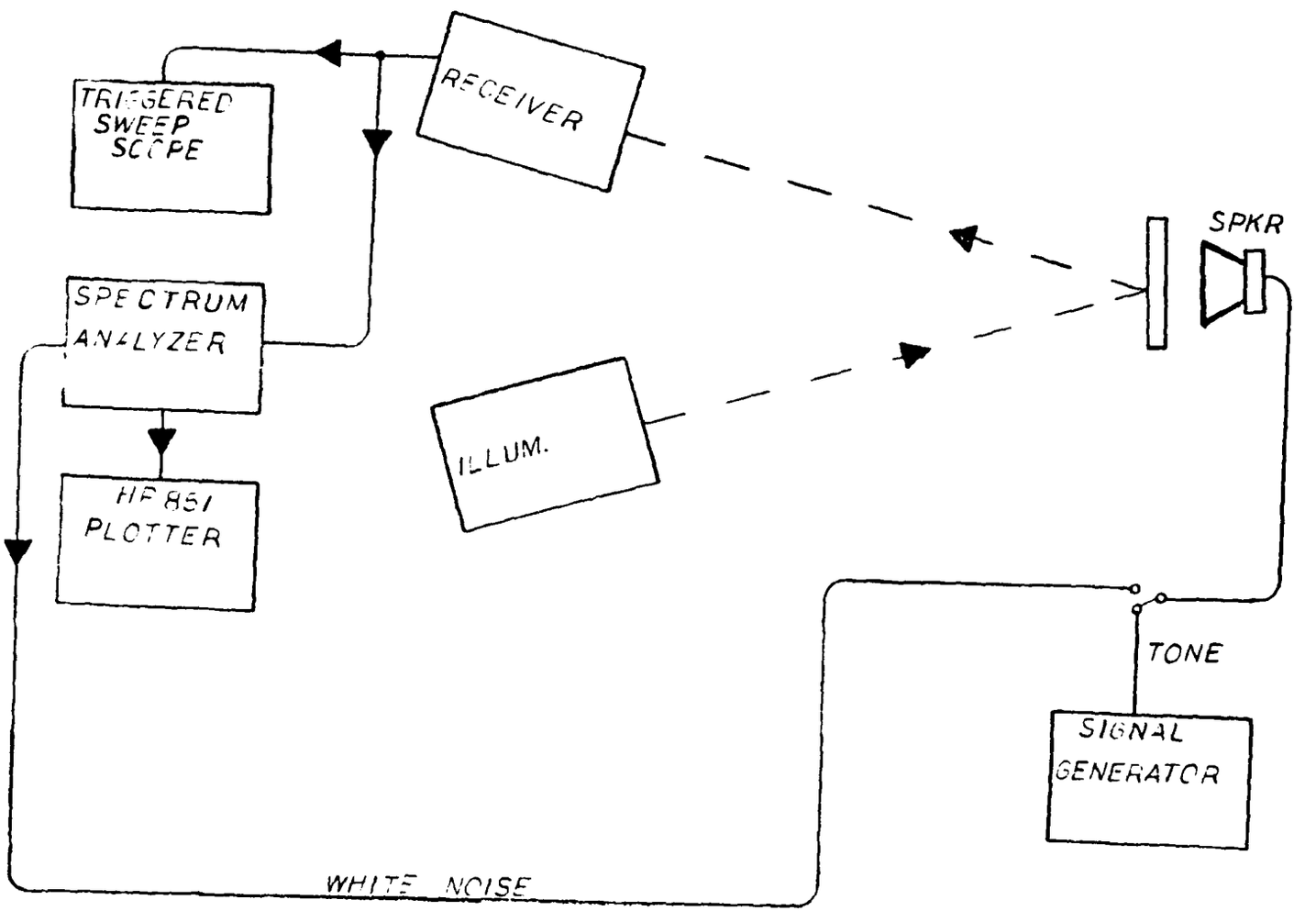

Figure 4. System Layout

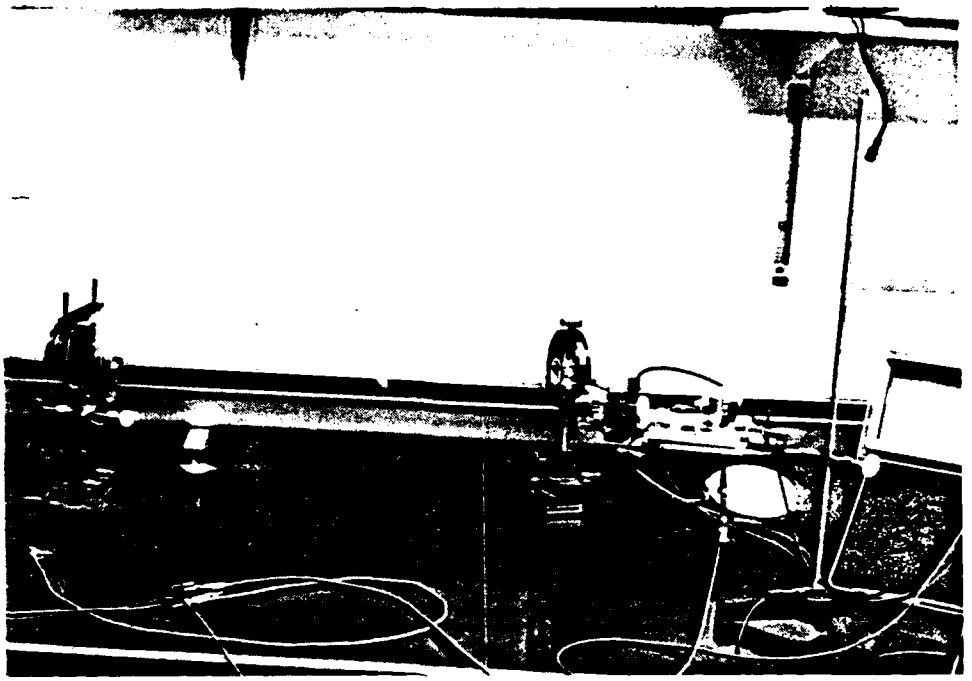

Figure 5. System layout (side view)

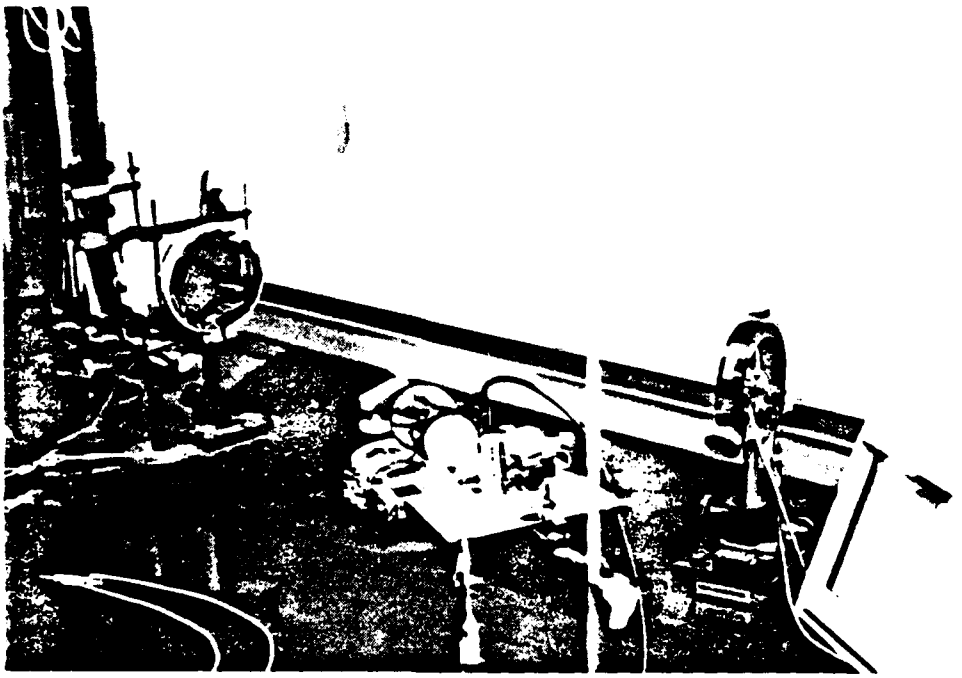

Figure 6. System Layout (receiver view)

excitation for the test object, the other source was an audio signal generator.

Figure 6 is another view of the system layout, taken from behind the receiver.

The test objects used in the initial tests were constructed by stretching various reflective materials over 100 mm embroidery hoops. Figure 7 shows the four test disks, and a twenty-five cent piece which was included for scale. The materials used were (clockwise from top) silver mylar sheeting, silver mylar painted flat white, transparent food wrap, and aluminum foil.

Figure 8 is a close-up of the transparent disk mounted in front of the speaker, in the test position. The bright reflection in the disk is that of the illuminator. Figure 9 is a side view of this arrangement.

To test the sensitivity of the receiver to specular and diffuse reflections the disk shown in Figure 10 was constructed of silver mylar, and then painted with flat optical white paint. Figure 11 shows the reverse of this disk, which was left in its normal state. By exposing either the silvered, or the flat white side of the disk to the receiver, comparative measurements could be made of the modulation capability of a diffuse and a specular reflector.

The illuminator was a commercial underwater flashlight lamp and reflector assembly mounted in an optical ring stand. The three-volt quartz-halogen bulb was powered by an

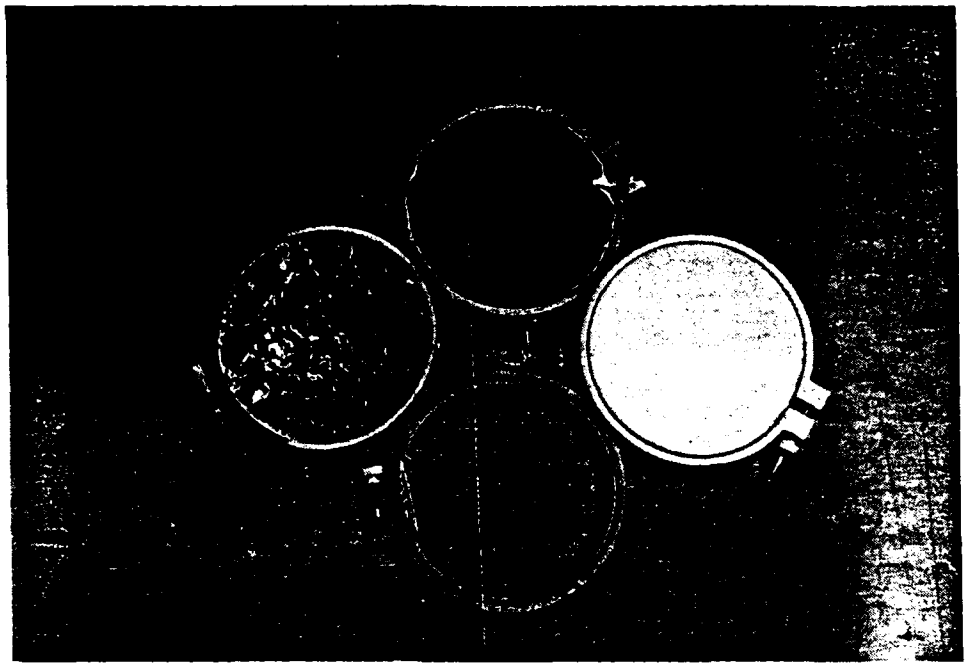

Figure 7. Test Objects (clockwise from top: Mylar, painted mylar, aluminum foil, plastic wrap)

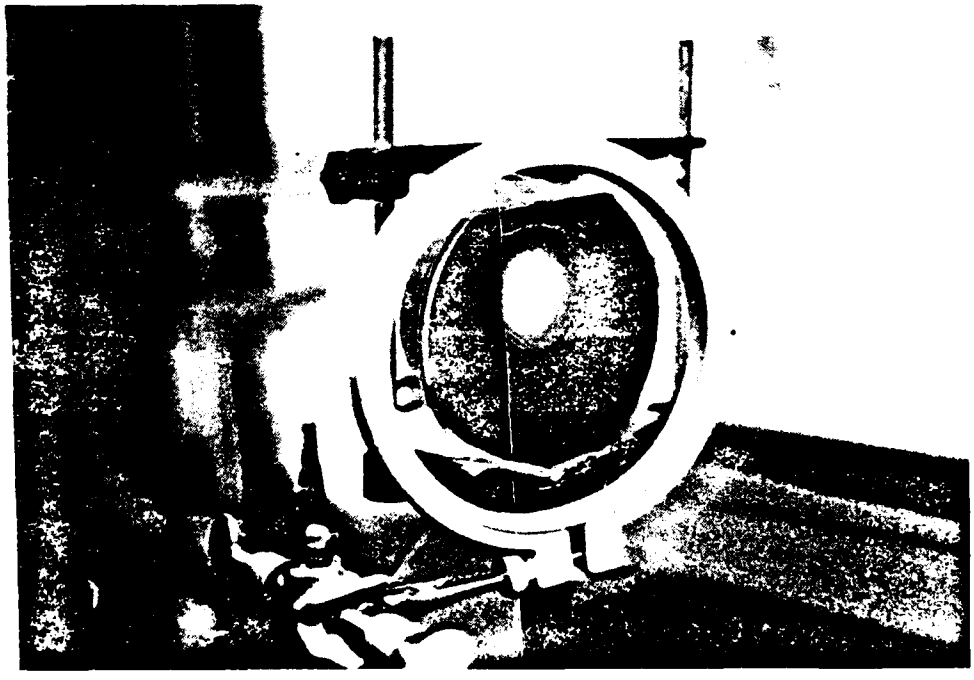

Figure 8. Disk and Speaker (front view)

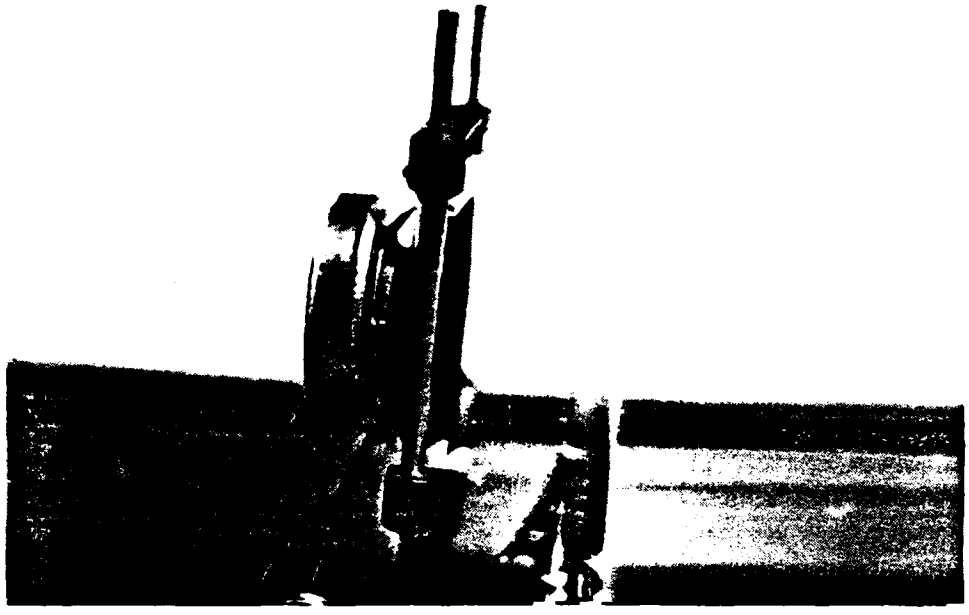

Figure 9. Disk and Speaker (side view)

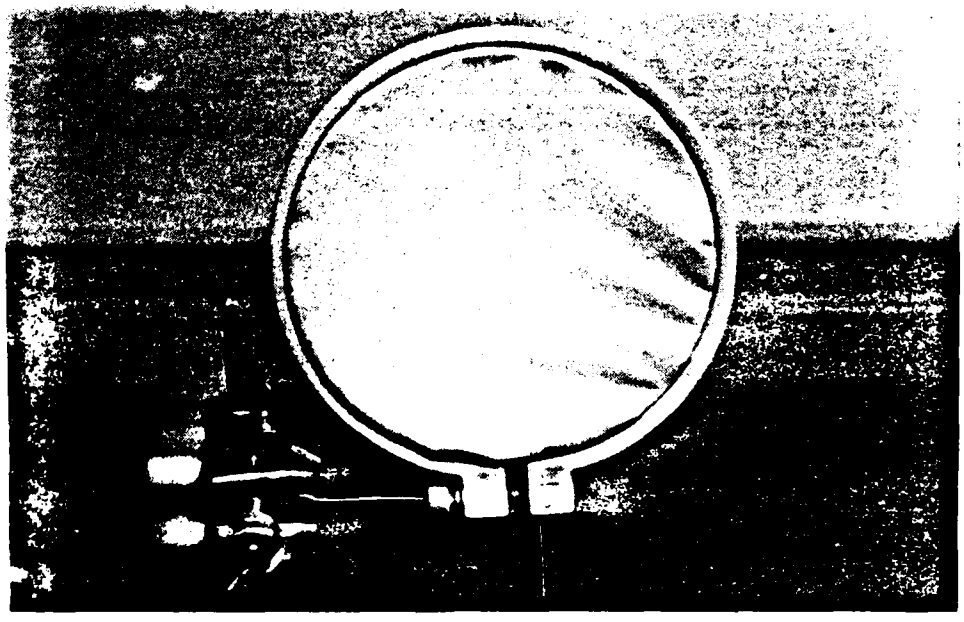

Figure 10. Diffuse/Specular Test Disk (diffuse side)

Figure 11. Diffuse/Specular Test Disk (Specular Side)

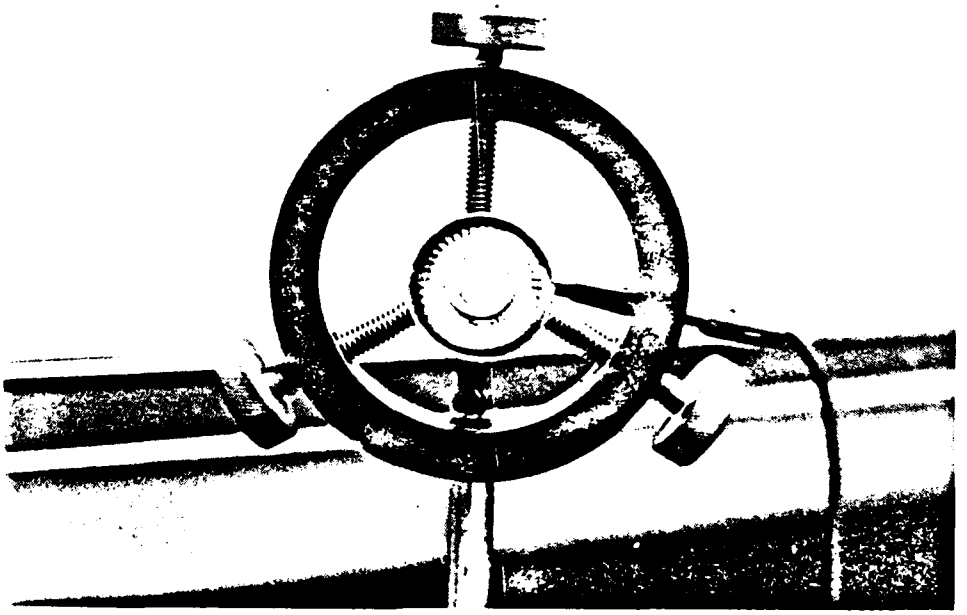

Figure 12. Target Illuminator

adjustable, filtered power supply to provide a variable sensing beam. Figure 12 shows a front view of the illuminator in operation.

The final piece of test equipment used was a battery operated sound pressure level meter, employed to measure the intensity of the acoustic excitation of the test object in some of the later experiments.

B. EXPERIMENTAL ENVIRONMENT

Initial tests of the receiver showed that it was highly sensitive to noise induced by AC powered fluorescent lamps and, to a lesser extent, AC powered incandescent lamps. The interference induced was highly regular; a 120 Hz spike for incandescents, and the addition of decreasing amplitude odd harmonics of this frequency for fluorescents. Although the predictability of the interference made it possible to account for it in the experimental results, the author elected to conduct all experiments in darkness to simplify interpretation of the results.

Another noise problem noted in the environment was that of acoustic noise. As will be explained in a following Chapter, some of the disks were extremely sensitive to external acoustic excitation. To prevent receiver clipping, the level of the excitation signal produced by the speaker was kept very low, generally just barely audible. Conversation, or the normal noises associated with a working laboratory, could be seen to be clearly influencing the test data. This problem

was suppressed by time averaging most of the data, which rejected the effects of transient noise. Impact spectra, collected from objects subject to mechanical impact, could not be time averaged, but since they were a result of fairly short (much less than one second) collection periods, they were not as seriously affected by local noise. Additionally, the high signal levels associated with the impact responses further suppressed this problem.

V. SYSTEM PERFORMANCE

A. INTRODUCTION

This Chapter presents the results of the experiments conducted in optical vibration sensing using AM detection. These tests evolved from several days of trial and error experimentation by the author, after the receiver was constructed and installed in the test layout. Although the remote sensing of impacts and the positive identification thereof in the presence of noise was of primary interest, some fundamental questions involving the nature of the induced AM needed to be addressed; hence such experiments as the diffuse / specular reflection signal-to-noise comparison.

The experiments are presented in the order they were performed, to give the reader a feel for the "top down" approach used in the investigation.

B. OBJECT IMPACT STUDIES

This series of experiments was conducted with the expectation of being able to remotely determine if an object had been impacted and, ideally, to identify the object from a small test population.

The experimental apparatus was arranged as shown in Figure 4, with the the speaker connected to the white noise source. Exciting the disks with white noise was expected to produce a signal at the receiver which was the convolution of the white

noise input and the response characteristics of the individual disks. Specifically, it was expected that the disks would all show peaks in their time averaged noise spectra corresponding to their mechanical resonance points.

The receiver and illuminator were trained on the test disk and the spectrum analyzer was used to produce a time average of 128 samples of the received signal. The resultant spectrum was inspected for each of the three test disks. This initial analysis showed that all the disks had multiple and distinct resonance peaks, and that the majority of these peaks lay in the region between zero and one kilohertz. With this knowledge in hand, further experimentation was limited to that region of the spectrum.

Each of the three disks was subjected to this bandlimited white noise excitation, and a plot of the characteristic resonance spectrum for each disk was produced. It was hypothesized that exciting a disk with a mechanical impact (instead of white noise) would produce a similar spectrum, which could then be used to identify the disk (based solely on matching the impact spectrum with the previously recorded white noise spectrum).

The test procedure is based on the assumption that an impact could be modelled as impulse excitation of the disk, and hence the acoustic response generated by an impact could be considered to be the impulse response of the disk. It is well known that the impulse (delta) function may be

practically replaced by its Fourier transfrom, i.e., white noise in filter impulse response studies, and this is frequently done as it simplifies the measurement of this important filter characteristic. (Although we are dealing with a mechanical filter in this case, the same principles apply.) Hence, we expect the white noise and impact spectra of the disks to be very similar.

The noise spectra recorded were normalized in the following manner: the sensor beam illumination was adjusted to produce a two volt (DC) output from the receiver front end with no acoustic excitation of the test object. The level of the white noise at the speaker was then adjusted to provide a strong signal at the receiver, just below amplifier clipping. This required markedly differing levels of both illumination and acoustic excitation for the three disks. (The differing levels of illumination required was not surprising, since one of the disks was transparent, and two were silvered. The differences in acoustic sensitivity were interesting however, and a separate experiment was designed to quantize this.)

Once these spectra were recorded, the speaker was removed and each disk was then subjected to a mechanical impact from a spring loaded plunger. (The impact was varied in its intensity for each case to prevent amplifier overload.) These impacts were analyzed using the transient capture mode of the spectrum analyzer, in which a signal sufficient to exceed the threshold preset on the instrument initiates a

single sample of the data and a subsequent display of its spectral components. This spectrum was then plotted for comparison to the previously obtained noise responses of the disks.

The results were encouraging. Figures 13 through 18 are the noise and impact spectra for the three test disks. The arrows indicate a visual correlation between the impact and noise spectra of a given disk. For example, the white noise excited spectral peaks for the aluminum foil disk (shown in Figure 13) located at about 110, 250, 380, and 390 Hz were also evident in the impact spectra for that disk (Figure 14).

The interested reader may wish to remove these plots from the binding and overlay them to see the remarkable correlation between the noise and impact results. Another interesting exercise is to overlay the various noise spectra on one impact spectrum, and attempt to identify the various test objects. The author had little difficulty distinguishing the three test objects based on this simple visual correlation, which is an admitally crude technique. That it works, even on this limited test population, is a strong indicator of the potential of AM detection when coupled with more sophisticated (i.e. computer based) correlation methods.

The aluminium foil disk showed the highest visual correlation between impact and noise spectra, and the mylar the worst, although it too was identifiable.

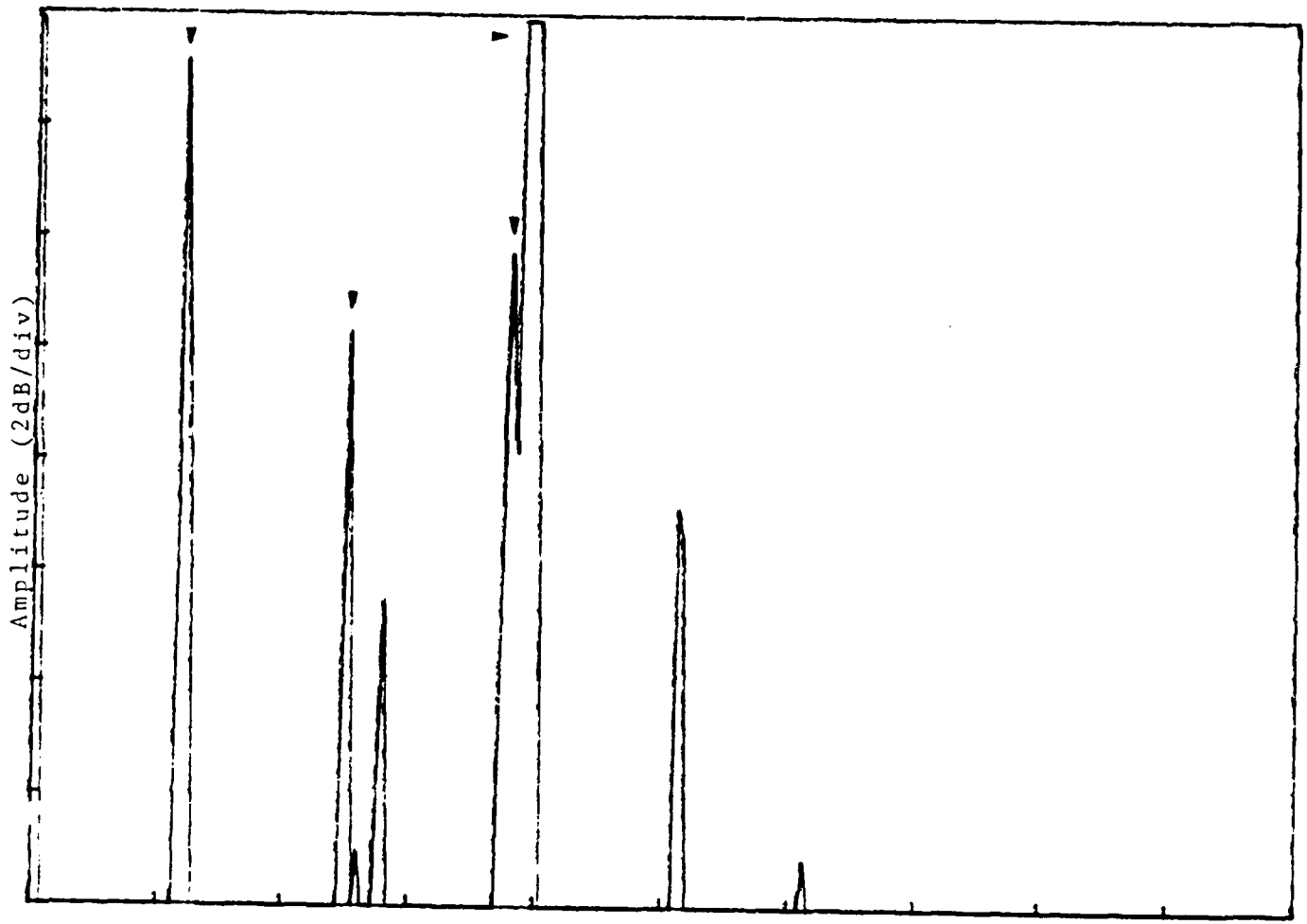

Figure 13. Aluminum Foil Noise Response

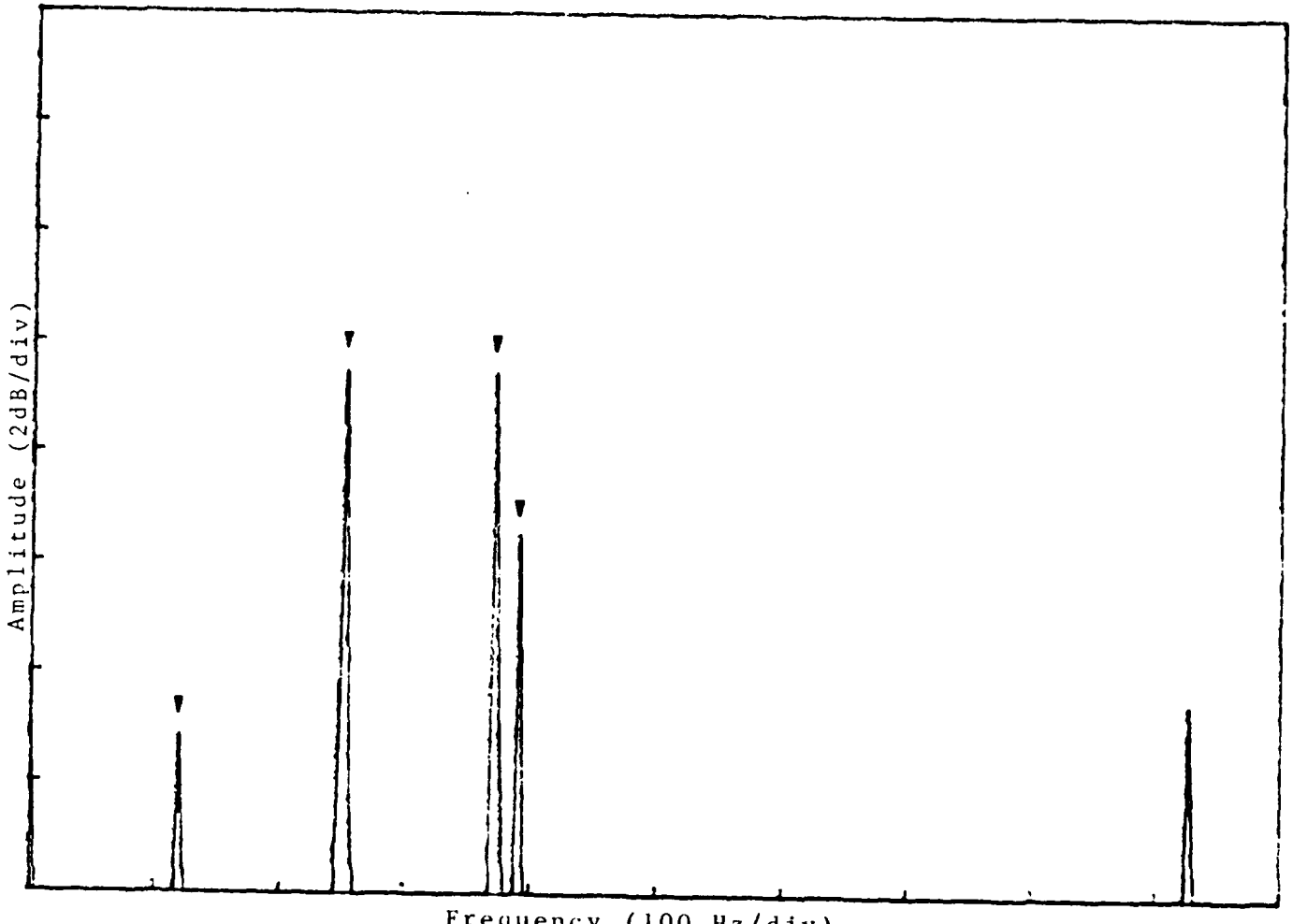

Figure 14. Aluminum Foil Impact Response

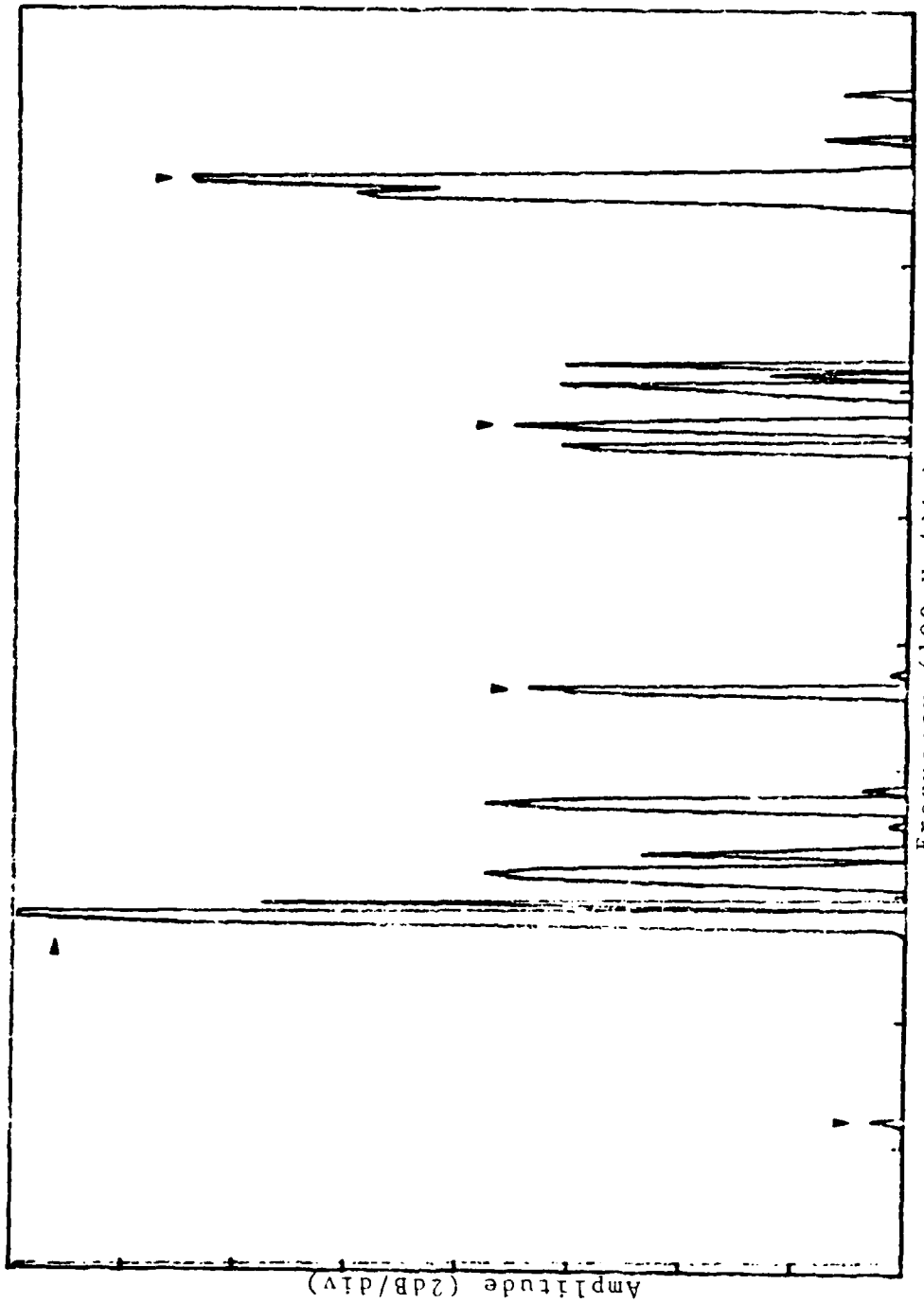

Figure 15. Plastic Wrap Noise Response

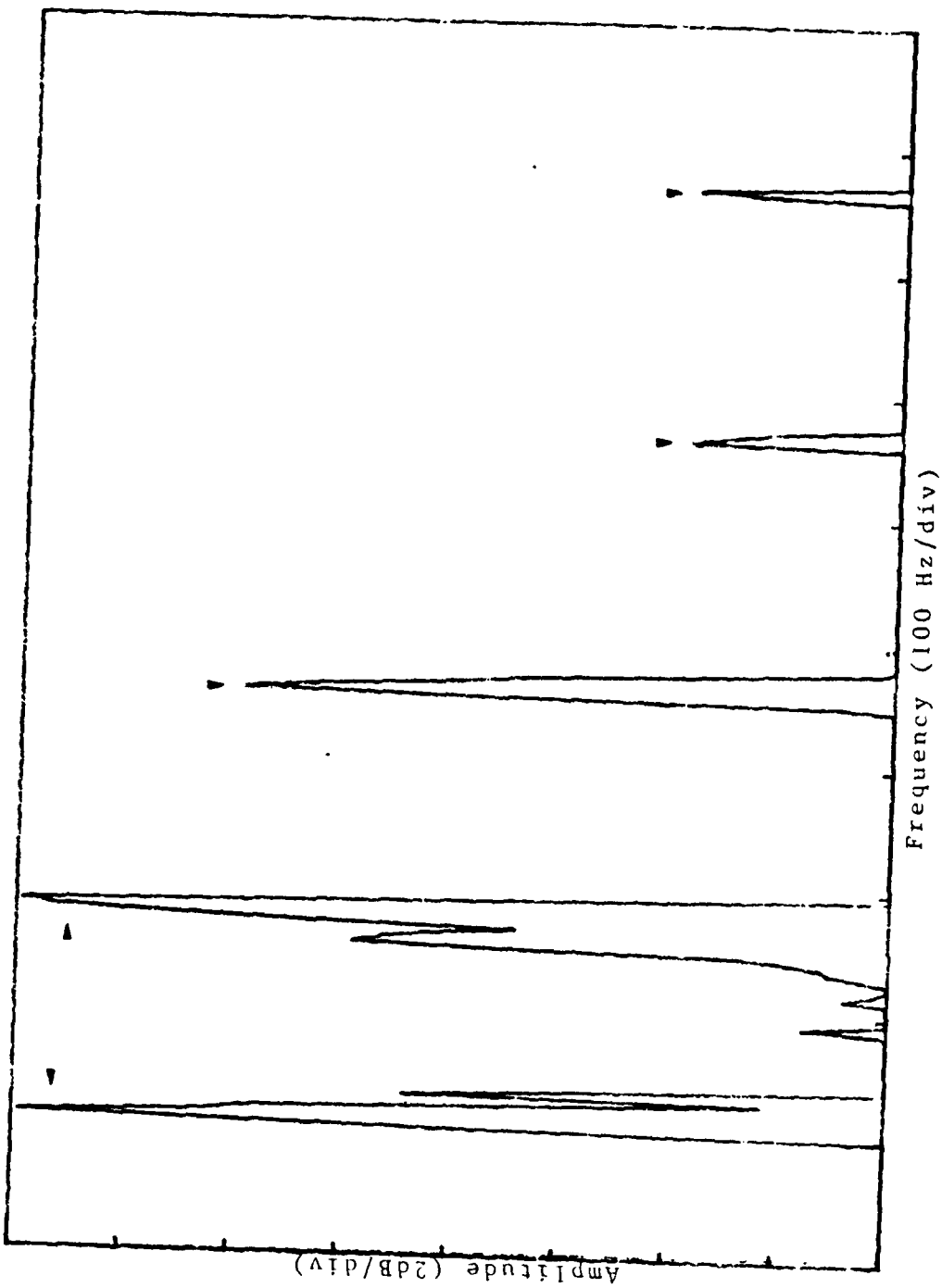

Figure 16. Plastic Wrap Impact Response

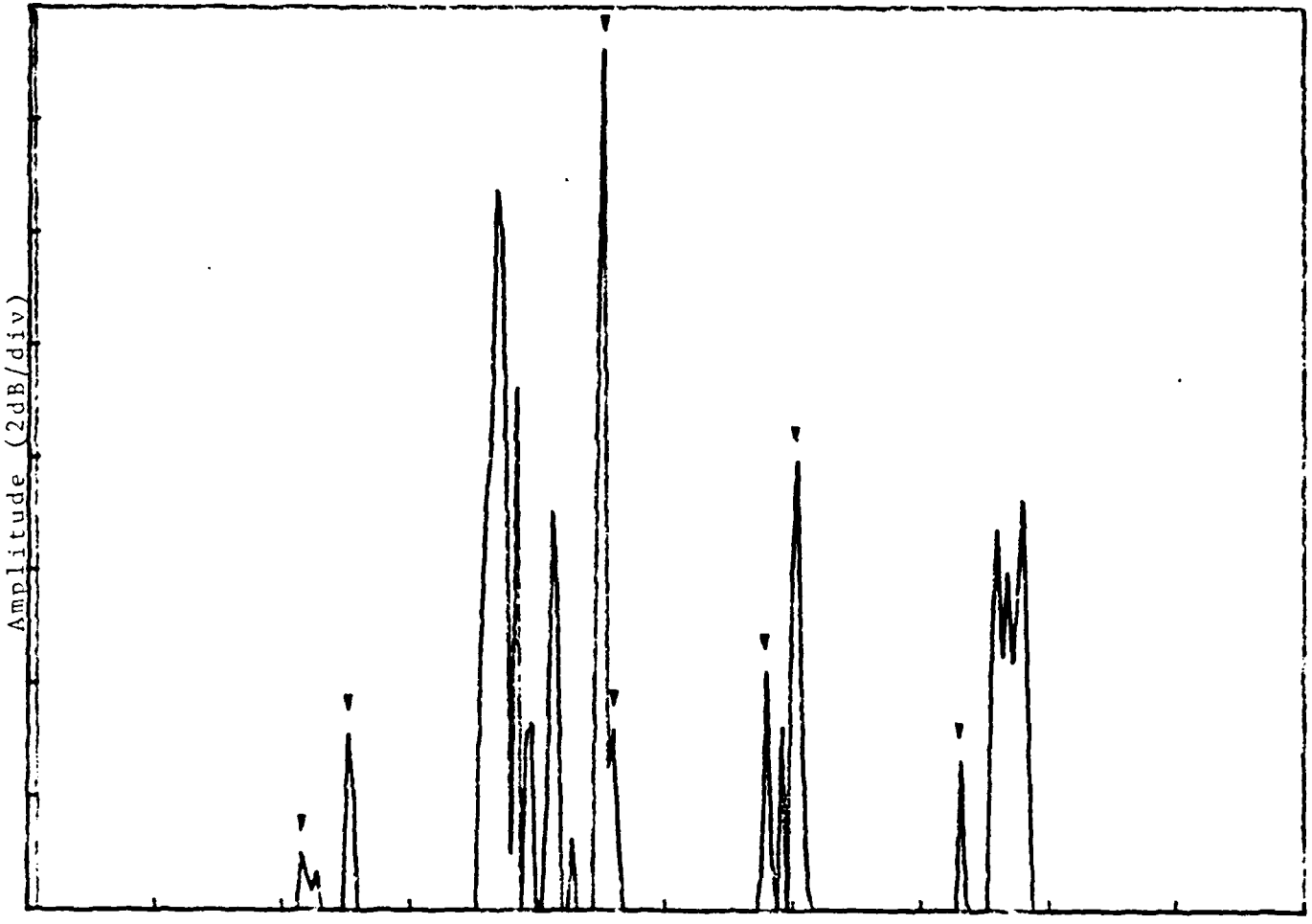

Figure 17. Mylar Noise Response

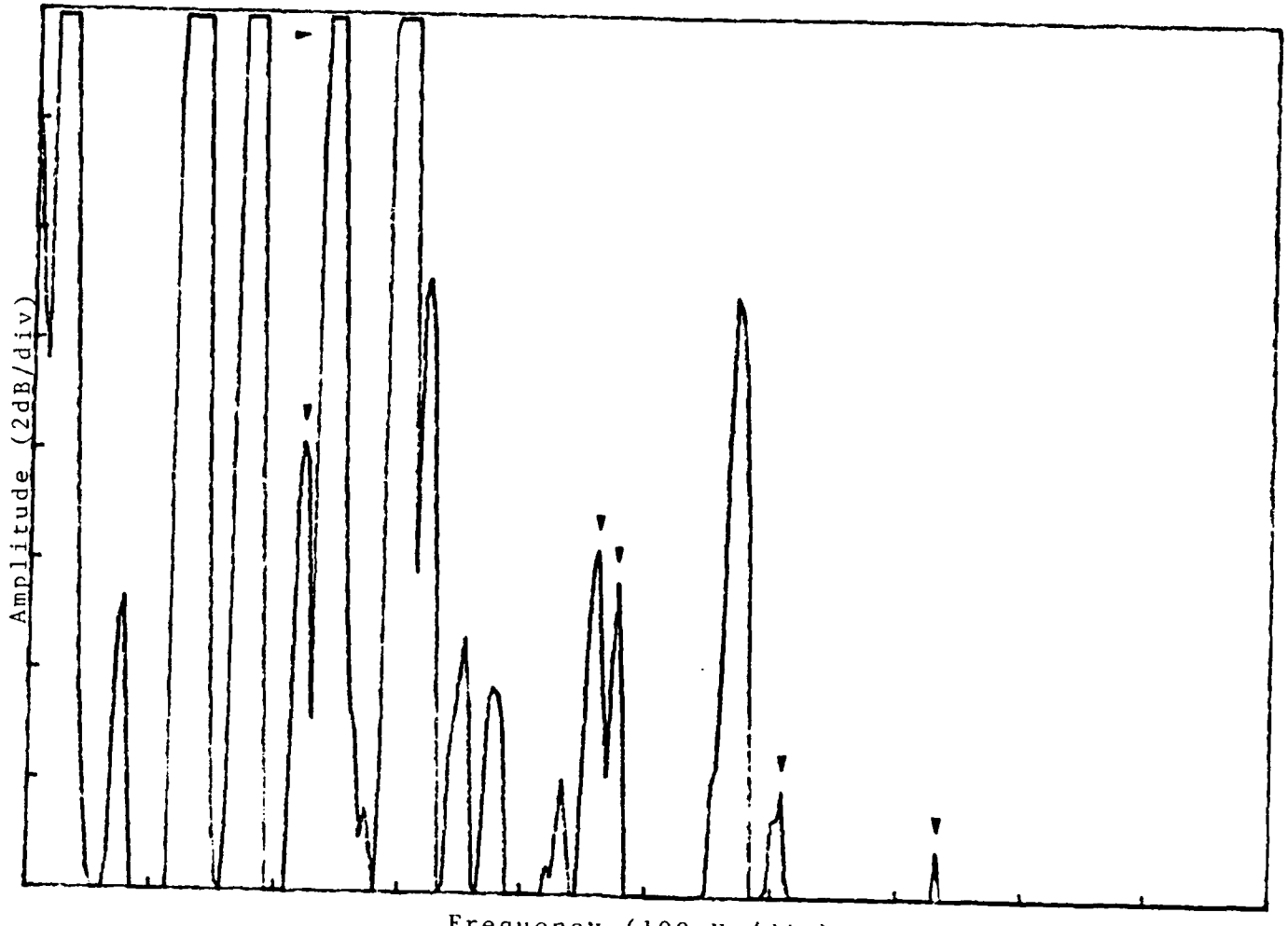

Figure 18. Mylar Impact Response

This fact did not come as a total surprise, since the noise spectrum peaks for the mylar were well below those of the aluminum foil (the aforementioned normalization masks this in the spectral plots). This indicates that the mylar is a better transducer in that it did not "color" the white noise to the same extent as the foil. Consequently, the white noise and the impact were both reproduced by the receiver with less coloring when the mylar was being tested, hence the spectral patterns were not as distinct at those of the aluminum foil. (Note the strong low frequency response of the mylar to impact, which is a result of its high compliance and sensitivity.)

C. COMPLEX OBJECT IMPACT

The above results seemed to indicate that the less compliant disks produced the spectra that were the easiest to identify. This suggested the next experiment wherein a geometrically complex metallic object was subjected to the same type of testing.

The test object chosen was an aluminum beverage can with an anodized, reflective finish. The can was mounted to the test stand by means of its lift tab, which was spot welded to the top. This provided a secure mounting, but one that did not tend to damp vibration in the main body of the can.

Although a rather high level of noise was needed, a noise spectrum for the can was obtained (Figure 19). The can was

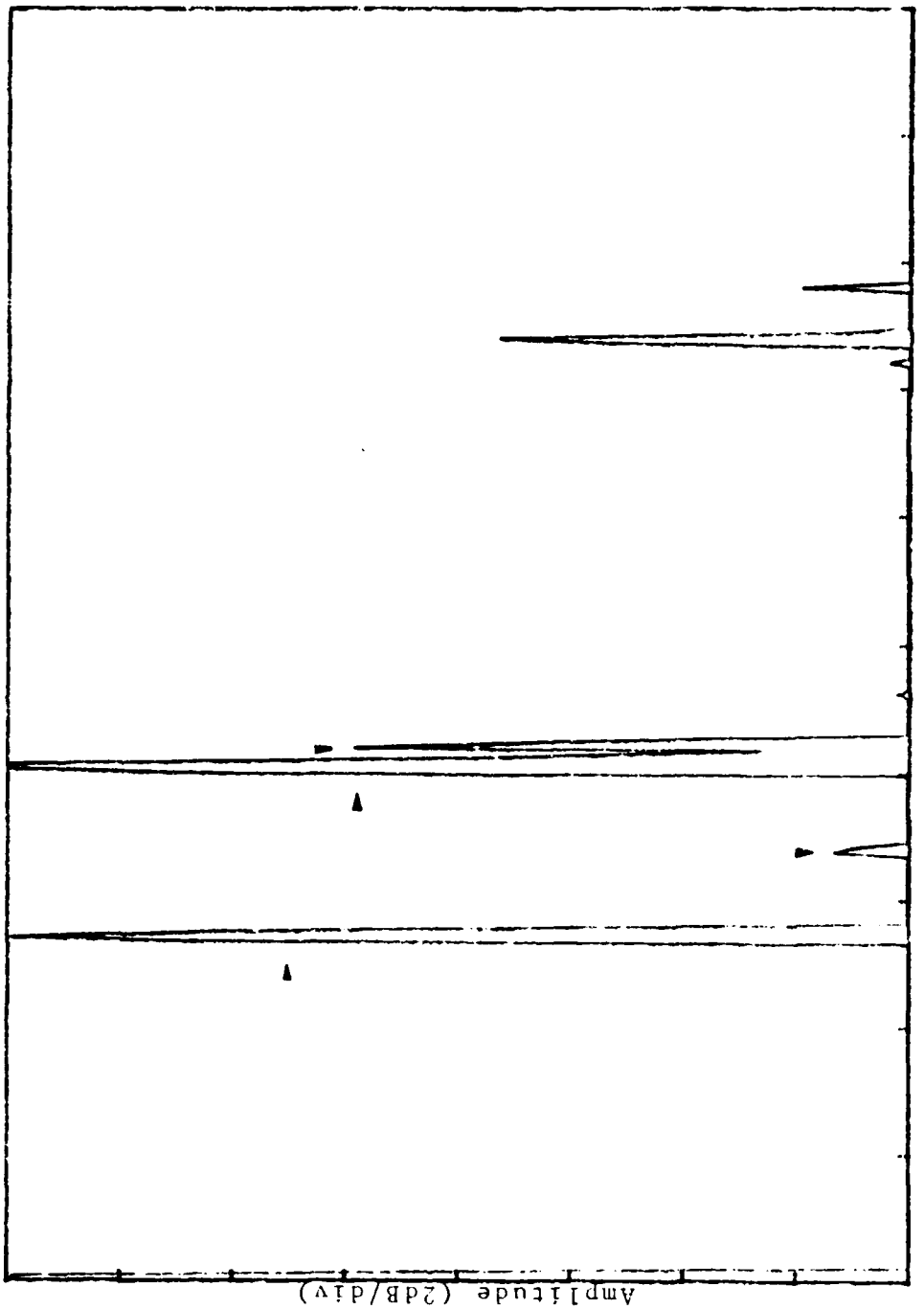

Figure 19. Cylinder Noise Response

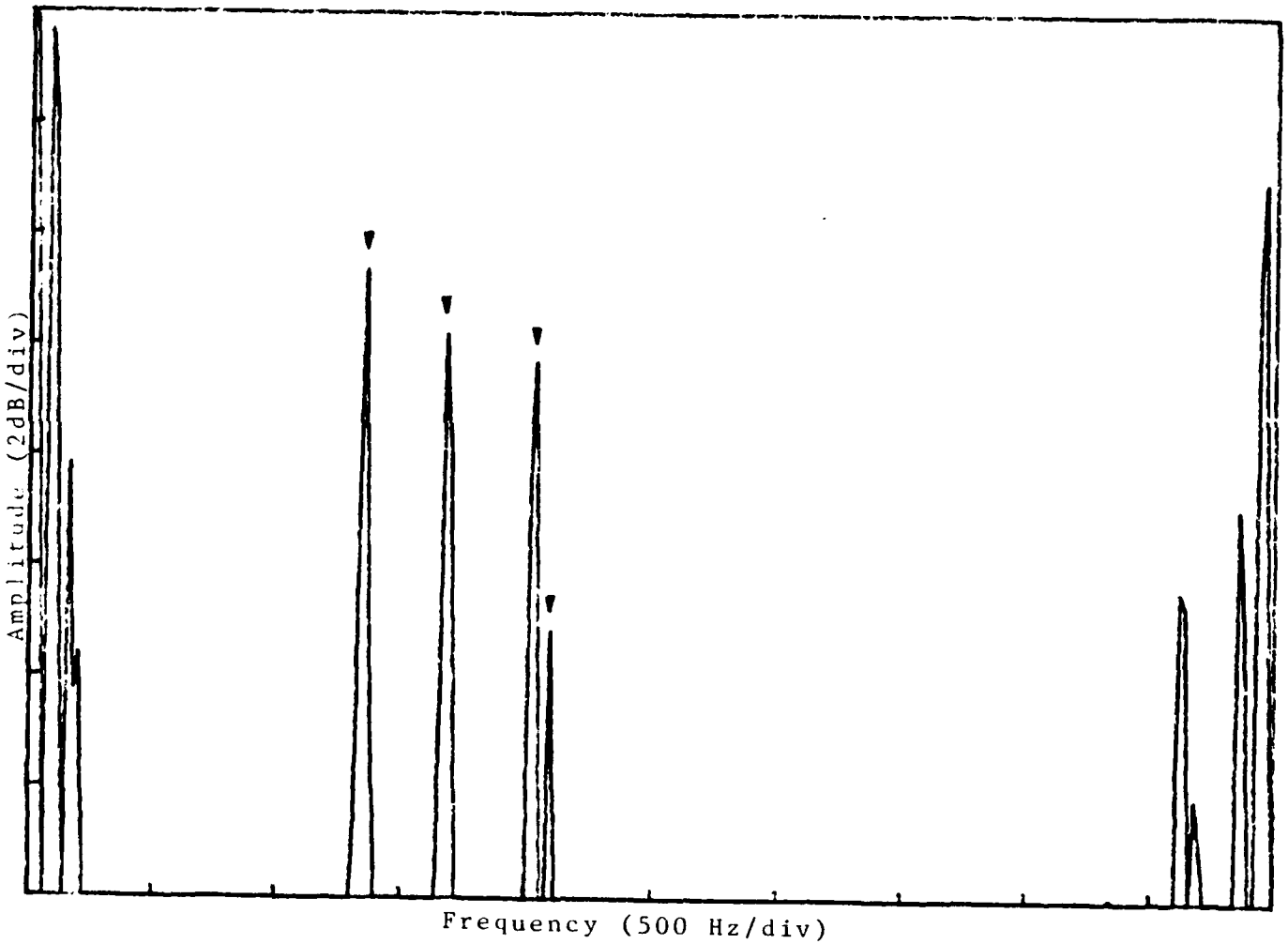

Figure 20. Cylinder Impact Response

then subject to a mechanical impact, and the resultant spectrum plotted. The impact was repeated on various surfaces of the can, and at varying intensities, however the results were always similar to those of Figure 20. It can be seen that four of the six noise spectrum peaks were clearly reproduced in the impact spectrum. (The low frequency components present in the impact spectrum were a result of the impact causing the entire can to vibrate on the test stand (at the weld joint of the tab) in addition to the normal "ringing".)

The "clean" noise and impact spectra produced in this case, and the obvious correlation between them, indicates that impact detection may be simpler against complex targets with strong, distinct vibrational modes.

D. COMPARATIVE TEST OBJECT RESPONSE TO NONRESONANCE EXTERNAL EXCITATION

As was mentioned in the previous section, the levels of acoustic excitation needed to produce a strong signal in the receiver varied widely for the three disks. An experiment was conducted to quantize these differences.

For this experiment, a new piece of equipment was introduced, the sound pressure level (SPL) meter. This device can give a standard SPL measurement of a given sound level using any of the three common weighting curves; "A", "B", or "C". The first two of these curves are tailored to match the response of the human ear, and are commonly used for industrial noise measurements by health and safety officials. The

so called dBC ("C" weighted) scale is an essentially flat decibel measurement of the incident sound pressure level, referenced to an arbitrary starting point of one dyne per square centimeter. (As a rough guide, a very quiet room will exhibit an SPL of about 55 dBC, and 120 dBC is considered to be the threshold of damage for human hearing.)

The experimental setup was again as shown in Figure 4, with the addition of the SPL meter, which was mounted in a fixed position near the speaker. The three disks were then excited with a single tone from the signal generator, and the SPL needed to produce a two volt peak-to-peak signal at the receiver output was measured for the three disks. The results are presented below, in Table II.

TABLE II

SPL COMPLIANCE TEST RESULTS

Disk	Receiver Output	Sound Pressure Level
Mylar	2.0 volts	75 dBC
Plastic Wrap	2.0 volts	81 dBC
Aluminum	2.0 volts	94 dBC

(Ambient noise 60 dBC)

The nearly twenty dB difference between the sensitivity of the Mylar and that of the aluminum foil points up the vast differences in these materials as transducers of incident acoustic energy. It is of interest that the ranking of these

materials, in best to worst order, is the exact opposite of their ranking in the previous experiment in noise/impact spectra correlation.

The frequency used to excite the disks for the above experiment was chosen at a nonresonance point for each one, as determined from the previously produced noise spectra. As will be discussed in the next section, the disks were much more sensitive to excitation at a resonance frequency.

E. RESONANCE SENSITIVITY OF THE MYLAR TEST DISK

While conducting the above experiment, it was noted that the output signal-to-noise ratio of the receiver could be made to vary widely by slowly sweeping the signal generator through the resonance peaks of the disk. Although certainly an expected effect, the high sensitivity of the Mylar disk to excitation at a resonance frequency was one of the more impressive demonstrations to casual observers. Using the layout of Figure 4, with a speaker-to-disk separation of 3 cm, a subaudible level of 500 Hz tonal excitation produced the input / output relation shown in Figure 21. The input to the speaker is shown in the top trace, and the output from the receiver in the bottom.

The interest generated by the fact that the excitation signal was inaudible to a nearby observer sparked a more careful measurement of this effect. Using acoustic excitation at the 520 Hz resonance peak of the Mylar disk, an SPL of only +7 dBC above ambient noise (measured at the disk's

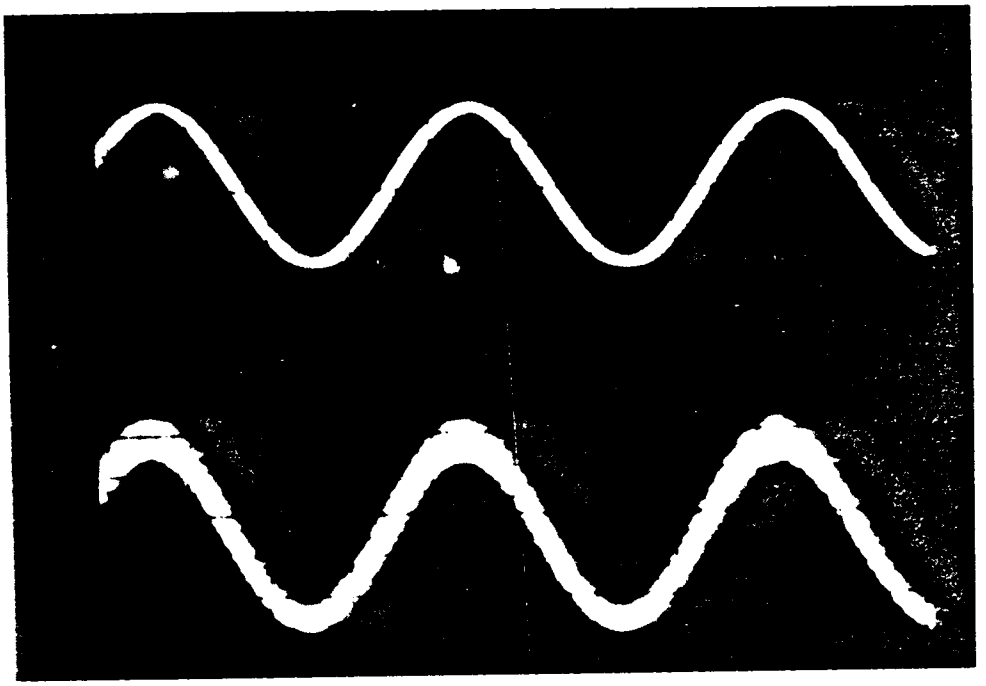

Figure 21. Typical receiver output (lower trace) in response low level audio excitation (top trace) of the Mylar target disk.

surface) produced a receiver signal 66 dB above the noise floor, as measured by the spectrum analyzer.

F. RECEIVER RESPONSE TO DIFFUSE AND SPECULAR REFLECTIONS

All three test disks used in the above experiments provided highly specular reflections. In an actual remote vibration sensor, particularly one designed for use against noncooperative targets, the operator might not be fortunate enough to get such a reflection of the sensing beam, or ambient illumination source as the case may be. This experiment was designed to measure the variability of receiver signal-to-noise ratio when viewing specular and diffuse reflections from targets exhibiting the same vibrational excursions.

For this test, the Mylar disk coated with flat white paint on one surface was used. As discussed in Chapter Two, and shown in Figures 10 and 11, this disk was only painted on one side leaving the other in its normal, specular silver state. This disk was mounted in the test stand with the silver side facing the receiver and illuminator. The receiver was aligned to directly intercept the reflected sensor beam, and the illumination power adjusted to give a no signal reading of 2 volts DC at the receiver front end. The signal generator was then connected to the excitation speaker, and its output was adjusted to give a moderate signal level at the receiver output (27 mv P-P). The SPL required to produce this output level was noted and the disk reversed on the mounting.

With the diffuse side of the disk now facing the receiver the sensor beam was, of course, not as efficiently reflected to the sensor. To compensate for this effect, the illuminator power was increased to provide the same no-signal DC level at the receiver front end as in the previous case (2 VDC). (The effect of this was to equalize the "carrier" strength for the two cases, so that the differences in modulation efficiency could be measured.) The signal generator was then adjusted to give the same receiver signal output as was produced from the specular side of the disk, and the SPL required to accomplish this was recorded. The disk-to-speaker distance was kept at a constant 3 cm in both cases. The results are presented in Table III.

TABLE III
DIFFUSE VS. SPECULAR REFLECTION SNR

Surface Type	Sound Pressure Level
Diffuse	43 dBC
Specular	7 dBC

(SPL shown is above a 61 dBC ambient noise level)

The large disparity in these figures shows that long range use of AM detection for OVS will be much easier against a specular target. This experiment also gives a clue to the underlying form of the modulation; a model based on the modulation being impressed by the physical sweeping of the

sensor beam (or subelements thereof) over the effective aperture of the detector fits well with these results. This sweeping action is a result of the physical distortions in the surface of the disk causing deflections in the sensor beam.

G. EQUIPMENT VALIDATION

An initial concern during the experimentation was that the resonance peaks shown in the various spectral displays were not a result of the vibration characteristics of the object under test, but rather were being impressed on the output by the other apparatus (receiver, speaker, etc.)

Overlaying the noise spectrum plots from the three disks showed no common frequency peaks, which implied that any system resonances were well below the levels of the disk resonances being measured. Further, the gain plot of the receiver amplifier showed no untoward dips or peaks over the audio frequency spectrum, which seemed convincing evidence that the receiver was not a likely source of system resonances. However, the speaker used as the noise excitation source, combined with its mounting, might have been. The following test was devised to examine this possibility.

The input of the spectrum spectrum analyzer was connected to the audio output of the SPL meter. (This output provides an audio signal from the SPL meter's calibrated microphone.) The white noise signal used to excite the test objects was then connected to the speaker, and the resulting signal from

the SPL microphone (placed 4 cm from the speaker) time-averaged over 512 samples. The spectral analysis (Figure 22) showed no peaks that could be consistently reproduced, indicating a lack of significant resonant points. The only repeatable feature of the spectrum was the smooth roll-off at the 200 Hz point, which was not unexpected for a 10 cm speaker.

To test whether a low level resonance would indeed be detected using this time-averaging of the SPL's output, the experiment was repeated but with a very low level 500 Hz tone injected into the environment near the speaker. This was done by placing the SPL calibration source (a small audio oscillator and transducer) in its 500 Hz tone generation mode, and physically mounting it beside the test speaker. The tone was adjusted to a point 9 dBC above the ambient background noise. The speaker white noise was then used to "bury" this weak tone, by adjusting its level to 24 dBC above ambient. A typical instantaneous (i.e. non time-averaged) spectrum of the resulting signal is shown in Figure 23. Note that the 500 Hz component is indistinguishable in the white noise.

The spectrum analyzer was then allowed to time-average the signal over 512 samples, as in the first test. The resulting spectrum (Figure 24) shows the 500 Hz tone reproduced quite clearly; hence it is to be expected that any significant

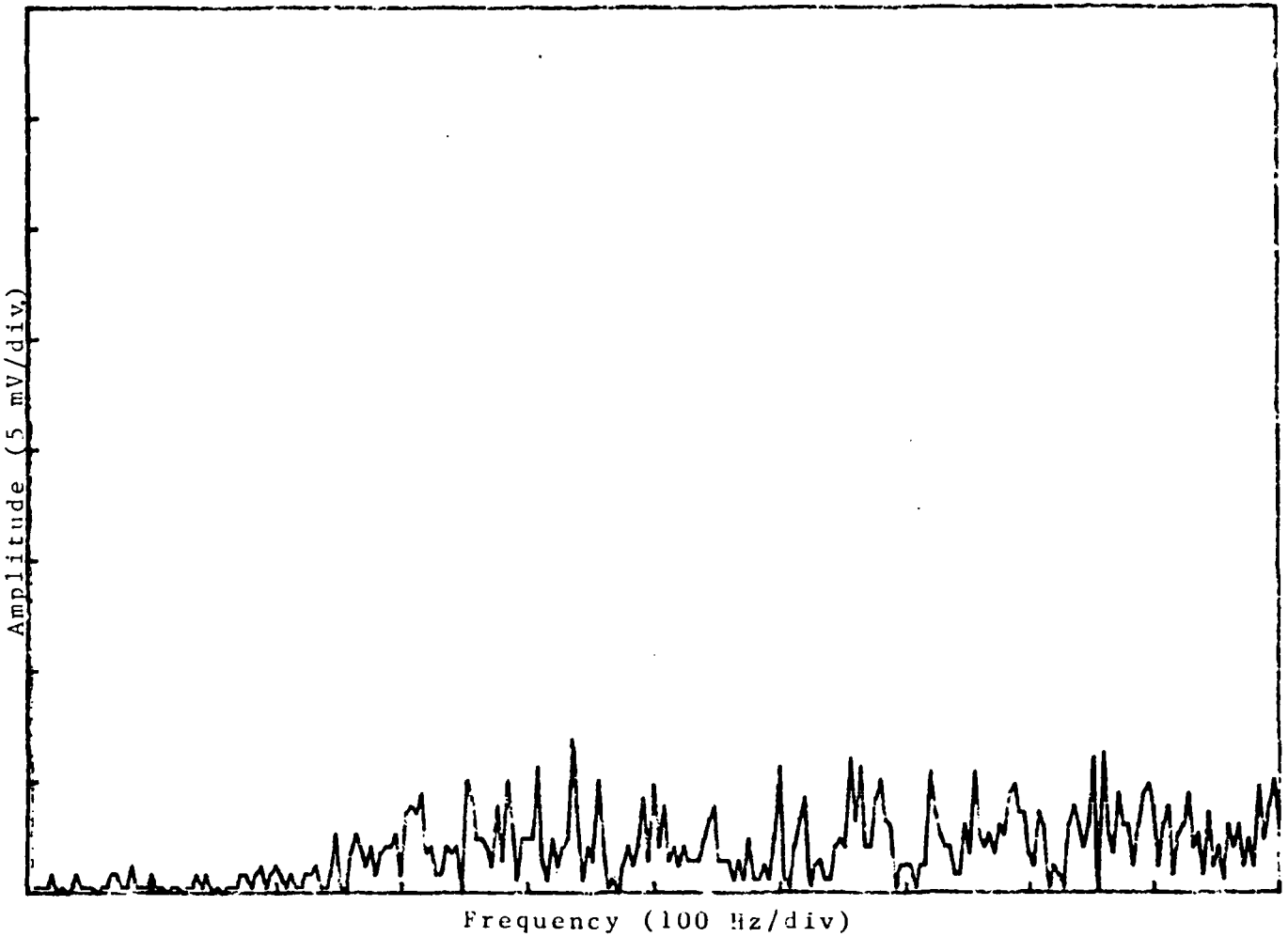

Figure 22. Speaker Noise Response (time averaged)

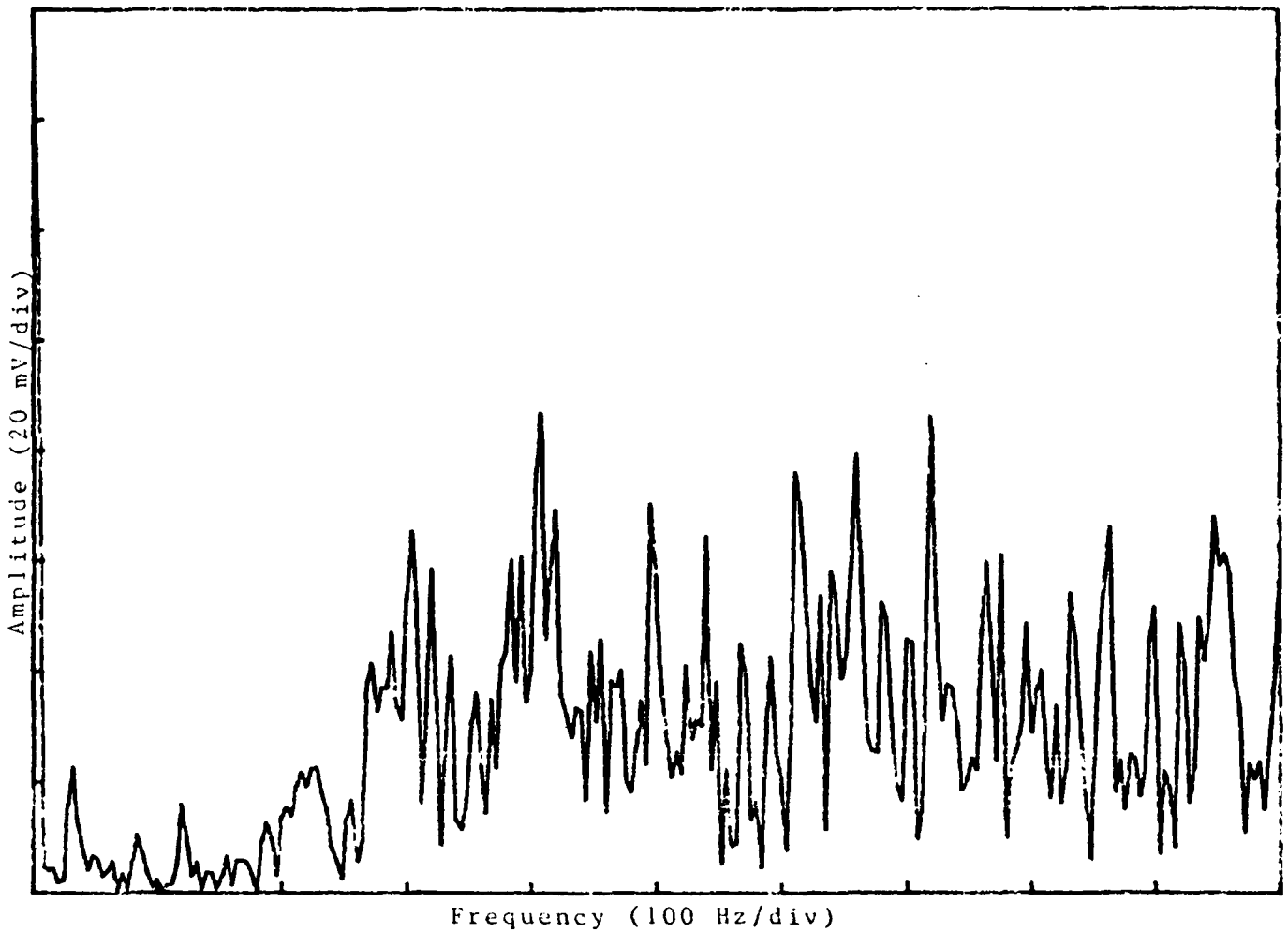

Figure 23. Speaker Noise Response + 500 Hz Tone (nonaveraged)

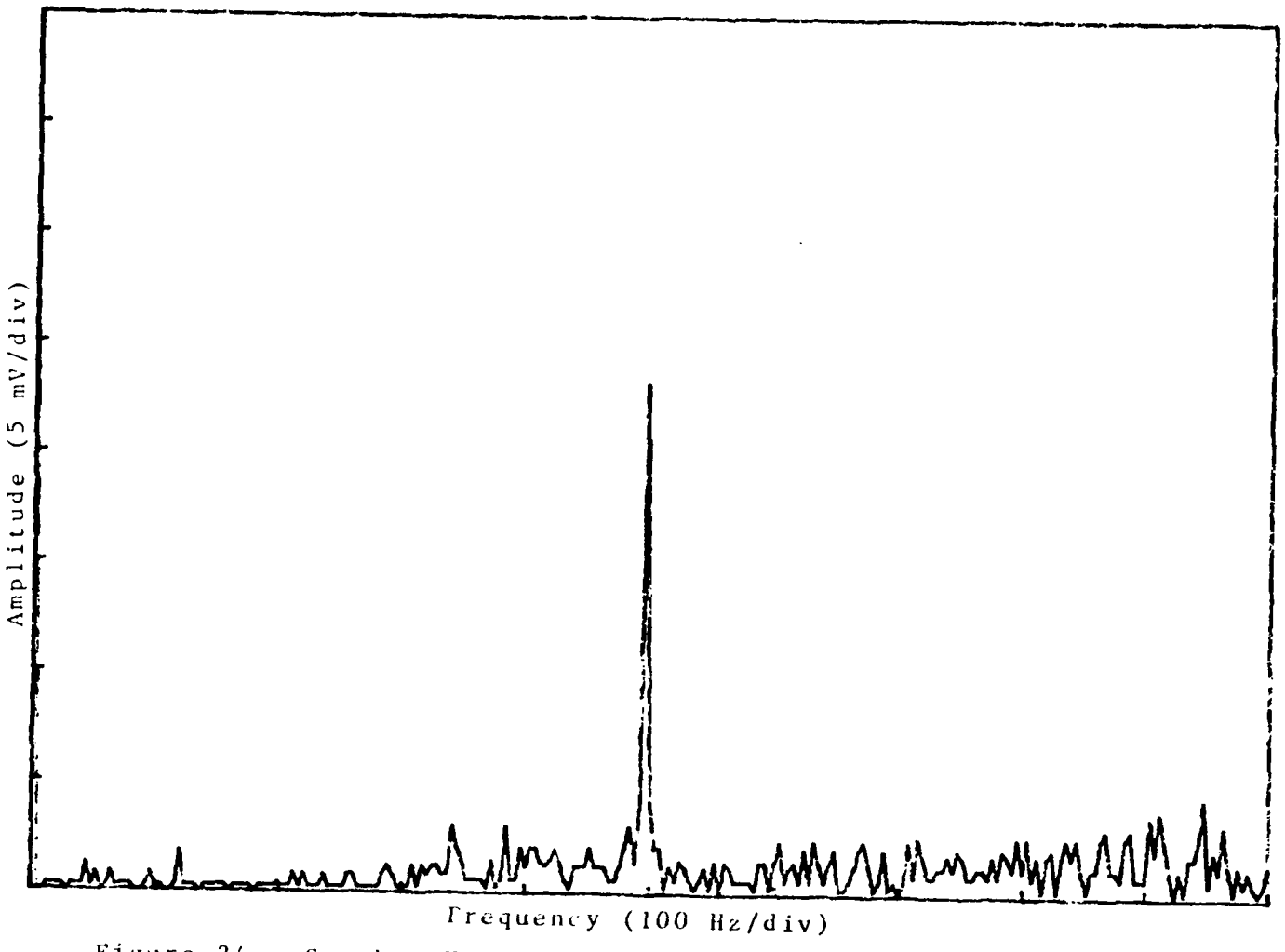

Figure 24. Speaker Noise Response + 500 Hz Tone (time averaged)

speaker or mount resonances would have indeed been detected by this type of measurement.

VI. THEORETICAL RANGE PREDICTION

In the Introduction to this thesis, the claim was made that AM detection for OVS could be exploited at long ranges, and against target glints resulting from reflection of ambient illumination. This chapter will develop a simplified prediction of the maximum range that such modulation detection could be accomplished, using the experimental transducer and lens assembly as a model.

To facilitate this development, several simplifying assumptions will be made. First, that the target and receiver are both in a vacuum, and hence there is no illumination scattered into the path between them. Second, the target is vibrating to such an extent that the entire reflected glint is swept across the detector's aperture (i.e. 100% modulation). Third, the target is being view against a perfectly black background, giving an infinite signal-to-noise ratio at the detector's input. Finally, only the signal-to-noise ratio at the output of the detector will be considered, any noise induced by further amplification will be ignored.

Although the above may seem to be simplification to the point of triviality, the expressions developed from this model do serve a useful purpose, much in the same manner as maximum radar range predictions based solely on the pulse repetition frequency; they give the maximum range that could

be expected under ideal conditions and serve as a basis for further modeling.

The SNR of the photodiode detector may be expressed as [Ref 6]:

$$SNR = \frac{\text{Responsivity (A/W) x Input (W)}}{\text{Noise Current (A)}} \qquad (1)$$

The responsivity of the detector used (TIL 413) may be computed as approximately 1.45 A/W (see Appendix A), and its noise current is specified as having a typical value of 5 nA. Hence, we may solve Equation 1 for the input power necessary to give a specified level of detector SNR at the output.

The maximum range that an optical sensing or communication system may be expected achieve is given by the optical range equation as [Ref 7]:

$$R^2 = \frac{P_O A_R t}{P_{TH} \theta^2} \qquad (2)$$

where:

R^2 = the square of the maximum range
A_R = the area of the receiving lens
t = transmissivity of the receiver optics
P_{TH} = the threshold receiver power
θ = the divergence of the sensor beam in radians
P_O = the power output from the target

"R" is, of course, the value to be computed, A_R is approximately 3.14×10^{-6} m^2 for the lens used in the experimental receiver. The value of "t" is not known precisely, but a value of .9 is generally taken as a good estimate in these

cases. P_{TH} is computed from Equation 1, given the detector SNR the engineer wishes to at the output.

The final two parameters may be estimated using the facts that the divergence of reflected sunlight is approximately the same as the angular width of the sun in the sky (about nine milliradians as seen from the earth) and that the solar flux at the top of the atmosphere is about 1350 watt/meter^2. Assuming that all of the spectral components of this radiation can be used equally by the detector (again an ideal case since the detector has a nonuniform spectral response), the last two parameters may be computed knowing only the target's reflective area, and its reflectance. Assuming the later to be unity, we may combine Equations 1 and 2 to obtain:

$$R^2 = \frac{(1350)(.9)(3.14\text{x}10^{-6})(d^2/4)(pi)}{(9\text{x}10^{-3})^2[(snr)(5\text{x}10^{-9})/1.45)]} \qquad (3)$$

where "d" is the target's diameter in meters (the target is assumed to be circular.)

Figure 25 is a plot of Equation 3, showing range (in kilometers) as a function of detector output SNR (in dB) for various target diameters. (Appendix B contains the computer program used to generate the data points plotted.)

Again it must be stressed that the above calculations are based on highly idealized circumstances. More accurate modeling of the environment in question, or empirical observation are needed to predict the exact range curves in a

given situation. One would, however, expect a form very similar to those shown in Figure 25.

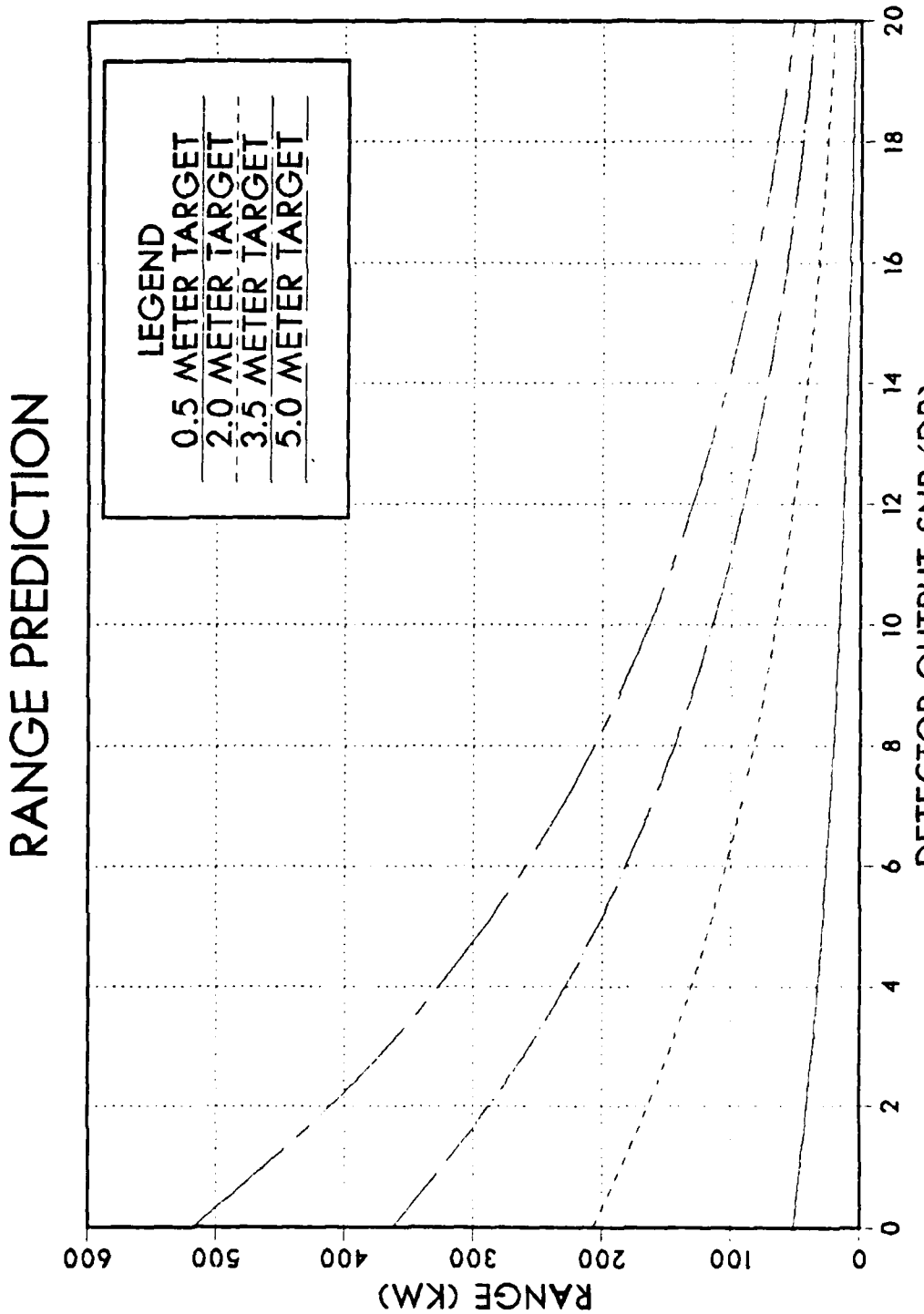

Figure 25. Theoretical maximum range curves

VII. CONCLUSIONS AND RECOMMENDATIONS

The use of AM detection as a method of optical vibration sensing was clearly demonstrated. This method easily recovers vibration frequencies in the audio spectrum, and shows respectable sensitivity when employed against specularly reflecting targets.

Noise, induced by a confused field of view for the sensor or as a result of atmospheric turbulence, would be expected to have a serious impact on this technique. Its effectiveness for impact detection may be impaired to a lesser extent than its effectiveness for vibrational analysis. This prediction assumes that the vibrational modes (tonals) of the object being scanned are known, or can be predicted. If this knowledge is available, then the well-developed arsenal of digital signal processing, as used in conventional sonar, may be employed to ease the signal-to-noise restrictions. The process of optically detecting an impact on a target (viewed against a noisy background) is very similar to that of long range detection of a submarine (in a noisy ocean) when taken in a signal processing context.

There are several other possible uses of this technology. For example, the Mylar test disk was reasonably sensitive, and had resonance peaks located well below those of the other materials. Presumably, using a suitably constructed

miniature disk of similar material, one could design a general purpose optical acoustic transducer. Similar in construction to a condensor microphone, the diaphragm would have little to impede its faithful reproduction of incident sound waves. However, unlike a condensor mike it could be "interrogated" over a range of tens of meters using very simple equipment. This would allow acoustic sensing in areas where it would be inconvenient, or impossible to route cables (in a sealed biological or nuclear containment vessel, for example). In a case such as this, the use of a monochromatic source such as a laser, and a narrow bandpass optical element at the receiver, such as an interference filter, could considerably reduce the optical background noise problem.

The noise induced in the receiver by fluorescent lights also brings up another possible use of the high gain optical receiver, an entirely passive one. The classification of ships by nationality could be assisted by using an AM receiver trained on a mastlight, or exposed internal light. The characteristic 50 or 60 Hz modulation recovered could be be of considerable aid in the identification process. Such a system could be easily employed from air, surface, or subsurface platforms.

The possibility of other modulations being impressed on such a signal are good, particularly for an incandescent lamp, whose filament is free to vibrate. The author noted such modulation in the experimental work for this paper. As

an example, scraping a fingernail across the ribbed outer surface of a flashlight (whose beam was directed at the receiver) produced a startlingly clear reproduction of the sound in the output of the receiver. Exploiting this phenomena, one might derive much useful information from a light source mounted rigidly on a target of interest.

Any of these topics might provide an investigator with an area of interesting research, however they also point up an important fact. The sources of "noise" that caused the abandonment of AM as a useable scheme for optical communication may all serve some measurement or sensing purpose if isolated and quantified in some manner. This research has primarily focused on the remote sensing of man-made effects, however the researcher in the biological or physical sciences may find equally useful "noise" sources to exploit, be it insect bioluminescence or lighting strokes.

APPENDIX A

TIL413 PHOTODIODE SPECIFICATIONS

Active Area:	4.4 mm^2
V_{BR}:	30 volts
I_D:	5 nA
I_L:	15 uA for 250 uW/cm^2 irradiance (930 nm)
C_T:	15 pF at V_R = 3 volts

This diode is mounted in a black, infrared transmissive plastic package of dimensions 6.5mm x 5.2mm. The front of the package is formed into a spherical lens with a radius of curvature equal to 2.5mm

APPENDIX B

COMPUTER SOFTWARE

I. HP-85 / HP-3582 / HP-7470 INTERFACE PROGRAM

```
10  !program transfers display from the 3582, including alpha-
     numerics, to the 85 display
20  !program can hardcopy to the HP-85 printer or plotter on
     HPIB
40  dim a$[520], b$[128], a(255)
50  iobuffer a$   ! display buffer
60  output 711 ; "HLTLFM,74400,256"
70  transfer 711 to a$ fhs ; count 512   !store display in a$
80  output 711 ; "LAN"
90  enter 711 ; b$ ! store display annotation in b$
100 output 711 1 "LFM,77455,1"
110 enter 711 using "#,B" ; c,d  ! single / dual channel input
120 s=250  ! single channel
130 plotter is 750 ! use plotter for hardcopy
138 k=40
140 limit k,k+178,k,k+127  ! plot size setup
150 pen 2
160 scale 0,s,0,1030
170 for i=255 to 0 step -1
180    enter a$ using "#,W" ; a(i) ! transfer display to "a"
190 next i
200 move 0,0
210 for i=0 to s  ! plot graph
220    a=binand(a(i),1023) ! remove non display data
230    plot i,a
240 next i
247 scale 0,100,0,100
250 xaxis 0,-10
260 yaxis 0,-10
520 print b$[1,32]   ! print annotations
530 print b$[33,64]
540 print b$[65,96]
560 print b$[97,128]
600 frame
610 disp "NOTATION ?"
620 input p$
630 print p$
700 pen 0
710 output 711 ; "RUN"
720 end
```

II. RANGE PREDICTION PROGRAM

```
10 REM   program to compute expected OVS range as a
20 REM   function of target size and detector SNR
30 REM
40 REM   george r. scott              sept 1985
50 REM
60 DEFINT I-N : DEFDBL R : IFILE=0
70 CL$=CHR$(26)  ' clear screen character
80 PRINT CL$;"Range Estimation Program"
90 PRINT : PRINT "Input upper,lower SNR bounds (dBW) and step: ";
100 INPUT SU,SL,SS
110 PRINT : PRINT "Input upper,lower target diameter (meters)
                  and step: ";
120 INPUT DU,DL,DS
130 REM
140 REM  begin computation loop
150 REM
160 FOR D=DL TO DU STEP DS
170    AR=(D*D)*(.785398)  ' compute area from diameter
180    FOR S=SL TO SU STEP SS
190       SF=(10^(S/10))  '  change dB to fractional form
200       R= (1.36659E+10 * AR) / (SF)  ' compute range
210       R=R^.5 / 1000   ' convert to kilometers
220       IF (IFILE)  THEN PRINT #1, USING "####.###!";S;",";D;",";R
230       PRINT USING "####.###"; S,D,R:PRINT
240    NEXT S
250 NEXT D
260 IF (IFILE)  THEN CLOSE : STOP
270 PRINT: PRINT "done"
280 PRINT "Repeat with file output ";
290 INPUT AN$
300 IF MID$(AN$,1,1)="y" OR MID$(AN$,1,1)="Y" THEN GOTO 320
310 STOP
320 PRINT "Name of file ";
330 INPUT FI$
340 OPEN "O",1,FI$
350 PRINT CL$ : IFILE=-1 : GOTO 160
```

REFERENCES

1. O'Shea, D. C., Callen, W. R., and Rhodes, W. T., Introduction to Lasers and Their Applications, Addison-Wesley, 1978.

2. Mims, F. M., Light Beam Communications, H. W. Sams, 1975.

3. Hampshire, E. W., A Wideband VHF Analog Intensity Modulated Fiber Optic Link, MSEE Thesis, Naval Postgraduate School, Monterey, California, June, 1977.

4. Richards, I. R., "Photoelectric Cell Observations of Insects in Flight", Nature, pp. 128-129, January 15, 1955.

5. Rodgers, G. L., Noncoherent Optical Processing pp. 9-10, Wiley & Sons, 1977.

6. Hewlett Packard Corporation, Optoelectronics Designers Catalog, page 500, 1983.

7. Campbell, R. W. and Mims, F. M., Semiconductor Diode Lasers, pp. 185-186, H. W. Sams, 1972.

INITIAL DISTRIBUTION LIST

	No. Copies
1. Defense Technical Information Center Cameron Station Alexandria, Virginia 22304-6145	2
2. Superintendent Attn: Library, Code 0142 Naval Postgraduate School Monterey, California 93943-5100	2
3. Professor J. P. Powers, Code 62Po Department of Electrical Engineering Naval Postgraduate School Monterey, California 93943-5100	1
4. Professor A. E. Fuhs, Code 72Fu Space Systems Academic Group Naval Postgraduate School Monterey, California 93943-5100	1
5. Naval Security Group Support Activity GX ATTN: LT George R. Scott 3801 Nebraska Ave. N.W. Washington, D.C. 20390	3
6. Naval Security Group Headquarters G-80 3801 Nebraska Ave. N.W. Washington, D.C. 20390	1
7. Naval Oceans Systems Center Electro-Optics Division Code A2500 San Diego, CA 92152	1